Preparation and Characterization of ZnO Nano-structured thin films

Thesis submitted in partial fulfillment of the requirement for
The award of the degree of

Master of Technology
In
Materials Science and Engineering

Submitted by

Nagendra Pratap Singh
Roll No.60602009

Under the guidance of

Dr. K.K.Raina
Prof. & Deputy Director
Thapar University, Patiala, Punjab, INDIA

Dr. V.N. Kulkarni
Professor, Department of Physics
IIT Kanpur, U.P., INDIA

School of Physics & Material Sciences
Thapar University, Patiala
Patiala - 147001

June-2008

CERTIFICATE

This is to certify that the thesis work entitled **"Preparation and Characterization of ZnO Nano-structured thin films"** submitted by **Mr. Nagendra Pratap Singh** in the partial fulfillment of the requirement of the award of the degree of M.Tech. in Materials Science and Engineering from the School of Physics and Material Science, Thapar University, Patiala (Punjab) is a record of candidates own work carried out by him under my supervision and guidance. The matter embodied in this thesis has not been submitted in any part or full to any other university or institute for the award of any degree.

Supervisor

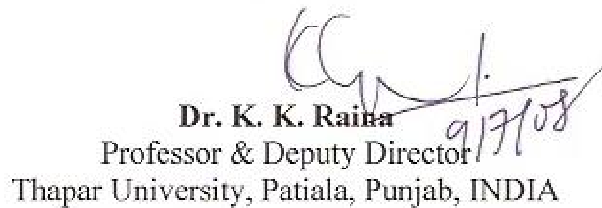

Dr. K. K. Raina
Professor & Deputy Director
Thapar University, Patiala, Punjab, INDIA

Countersigned by,

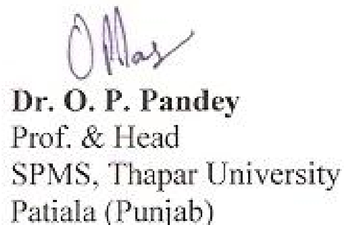

Dr. O. P. Pandey
Prof. & Head
SPMS, Thapar University
Patiala (Punjab)

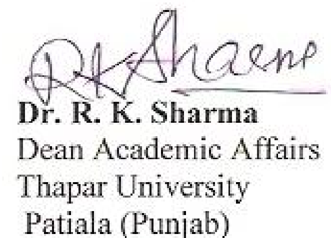

Dr. R. K. Sharma
Dean Academic Affairs
Thapar University
Patiala (Punjab)

Indian Institute of Technology Kanpur
Department of Physics

Dr. Vishwas N. Kulkarni
Professor of Physics,
IIT Kanpur
Kanpur-208016 (India)

Phone: +91 (512) 2597985 (O),
2598687(R)
Fax: +91 (512) 2590914
E-mail: vnk@iitk.ac.in

JULY 7, 2008

CERTIFICATE

This is to certify that the thesis work entitled ***"Preparation and Characterization of ZnO Nano-structured thin films"*** *submitted by* ***Mr. Nagendra Pratap Singh*** *in the partial fulfillment of the requirement of the award of the degree of M.Tech. in Materials Science and Engineering from the School of Physics and Material Science, Thapar University, Patiala (Punjab) is a record of candidates own work carried out by him under my supervision and guidance. The matter embodied in this thesis has not been submitted in any part or full to any other university or institute for the award of any degree.*

Supervisor

Dr. Vishwas N. Kulkarni
Professor
Department of Physics
Indian Institute of Technology
Kanpur-208 016 (India)

Acknowledgement

I visualize a rare movement of pride and pleasure to extend my sincere and heedful gratitude to my Guide Dr. K.K. Raina, Professor & Deputy Director, Thapar University Patiala (Punjab) and Dr. V.N. Kulkarni, Professor in Department of Physics, IIT Kanpur (U.P.) for not only providing me his inspiring and talented guidance but also his constant attention and constructive and healthy criticism throughout the time.

My greatest thanks are to Dr.O.P. Pandey, Prof. & Head, School of Physics and Material Science, Thapar University, Patiala for his valuable Suggestions and full motivation & appreciation in my research work and Dr. N. K. Verma, Dean Student Affairs Thapar University for their full motivation and appreciation to my work. They provide me moral support as well as necessary help during my experimental work.

I am highly greatful to Dr. Kulvir Singh, Asst. Prof. School Of Physics And Material Science, Thapar University Patiala (Punjab) for their kind help and valuable suggestions and special attention throughout my work. It is due to his moral encouragement, love and providing me fountain of inspiration all shorts of assistance from time to time into up-bringing me upto this stage.

I am also indebted to Dr. S. Damodaran Lecturer at Department of Physics, IIT Kanpur and Dr. Sunil Kumar, Dr. D.P. Singh, Dr.S.D.Tiwari, Dr.Sanjeev Das and all other faculty members in SPMS, Thapar University Patiala (Punjab) for their graceful and kind hearted support.

I would like to Special thanks to Dr.Inderpreet Kaur, Scientist, CSIO Chandigarh for her kind attention, providing me AFM facility and valuable suggestions during course of my work. My special thanks to Mr. Masood Sr. Technical Superintendent, and Mr. Rajnish Dhiman Sr. Technical Assistant, Central Nuclear Lab, IIT Kanpur.

I am unable to perform all the work without moral support of ***Dr. Pankaj Kumar.*** *My special thanks to* ***Mr. Purushottam K. Singh*** *for his assistance, comments and views were very insightful and helpful.*

I would also like to thank Dr. ***Hariprada Bhunia*** *for providing all kind of assistance in Chemical Engineering Lab for spectrophotometer facility.*

I would also like to give many thanks to Research Scholars ***Mr. Sarvesh Tripathi, Mr. Niraj Shukla, Ms Shikha Kapila, Ms. Neeraj Sharma , Mr. Ravi Kumar Shukla*** *and* ***Ms.Deepika Sharma, Mr. Ravi Prakash Srivastava*** *for any kind of help and valuable suggestions whenever I needed out of their busy schedule and valuable time.*

I am very much thankful to my father ***Late Sri R. S. Singh,*** *my mother* ***Smt. A. Singh,*** *my elder brother* ***Sri Rakesh Kumar Singh*** *who provides me mental and financial support for this Project work. I am also thankful to* ***Dr. D.P. Upadhyay*** *Reader in Geography VBS Purvanchal University, Jaunpur for providing me mental encouragement at the every time of work.*

Nagendra Pratap Singh

(Roll. No.: 60602009)

Date:...9/07/08

Place:...Patiala

ABSTRACT

Zinc Oxide has a wide range of properties that depends on doping, process parameters, fabrication methods and thickness of the thin films. The properties of zinc oxide include high transparency, piezoelectricity, wide band-gap semi-conductivity, room temperature ferromagnetism and huge magneto-optic and sensing properties.

We can obtain the different nano-structures of ZnO by changing the process parameters in thermal evaporation system. We have fabricated thermal evaporation system by designing and assembling the components to achieve high vacuum. We have achieved the vacuum of 10^{-6} m bar.

We have deposited ZnO thin film by taking ZnO powder (MERK 99.98%) and deposited on the properly cleaned glass substrate directly evaporating powder in the chamber. Deposited thin film was annealed at the temperatures 450^0C, 500^0C, 550^0C and 600^0C. The thickness and band-gap of the thin films was 334.09nm and 3.25eV measuring by UV/VIS Spectrophotometer. The XRD peaks reveal that the crystallinity improves with the annealing temperature. The surface morphology, surface roughness and adhesion properties have been studied by the Atomic Force Microscope (AFM). Adhesion property on glass substrate improves with annealing temperature. The grain size increases with increase in annealing temperature. The surface roughness changes with annealing temperature and observed highest at 550^0C (R_a=444.558nm) with RMS value 516.230nm.

Contents

	Page No.
Certificates	**i-ii**
Acknowledgement	**iii-iv**
Abstract	**v**
Contents	**vi-vii**
Lists of figures and tables	**viii-ix**
Chapter 1	
Thin Film: An Overview	1-20
1.1 Introduction	1
1.1.1 Properties of thin films	2
1.1.2 Thin film growth process	3
1.1.3 Epitaxy	7
1.2 Method used for deposition of thin film	8
1.2.1 Physical Vapour Deposition (PVD)	9
1.2.2 Chemical Vapour Deposition (CVD)	13
1.2.3 Chemical Solution Deposition (CSD)	14
1.3 ZnO the novel material	19
Chapter -2	
Synthesis and Experimental Techniques	21-41
2.1 Fabrication of Experimental Set-up	21
2.1.1 Fabrication of coupling arrangement of turbo pump to vacuum chamber	22
2.1.2 Fabrication of resistive heating arrangement of the material to be deposited	25
2.2 Deposition of thin film	27
2.2.1 Experimental Set-up used for ZnO thin film deposition	27
2.2.2 Materials Used	27
2.2.3 Methodlogy	28

	Page No.
2.2.4 Substrate Cleaning	30
2.2.5 Experimental Procedures	31
2.2.6 Annealing of samples	34
2.3 Charcterization Techniques	35
2.3.1 X-Ray Diffraction	35
2.3.2 UV/ VIS Spectrophotometer	36
2.3.3 Atomic Force Microscopy	38
Chapter –3	
Results and Discussion	42-50
3.1. X-ray Aanalysis	42
3.2. UV/ VIS Spectrophotometer Analysis	44
3.3. AFM Analysis	46
3.4 Conclusions	49
3.5 Future scope	50
References and Bibliography	51-53

Lists of Figures and Tables

List of Figures:

Figure-1.1: Thin film growth process (condensation)

Figure-1.2: Monolayer and Island growth process

Figure-1.3: Various steps in thin film growth process

Figure-1.4: Crystalline and amorphous structures of thin film

Figure-1.5: Influence of substrate temperature

Figure 1.6: Schematic representation of the classification of some of the common thin film deposition processes.

Figure 1.7: Electron Beam Evaporator

Figure 1.8: The schematic representation of the fundamental processes occurring during sputtering

Figure-1.9: Thin film deposition steps

Figure-2.0: Various stages of dip coating process

Figure-2.1: Sol-gel dip coating processes

Figure 2.2: Thermal Evaporator System Designed and Fabricated

Figure 2.3: Coupling arrangement with high vacuum valve

Figure 2.4: Butterfly valve

Figure 2.5: Ring for rotation of valve

Figure 2.6: Flanges with gauge head inlets

Figure 2.7: Flanges, which joins the pump

Figure 2.8: Resistive heating and other components arrangements

Figure 2.9: Thermal Evaporator fabricated at central nuclear lab IIT Kanpur

Figure 3.0: The Hexagonal wurtzite crystal Structure of ZnO.

Figure 3.1: Thermal Evaporator used for deposition

Figure 3.2: X-Ray reflection pattern

Figure 3.3: Ray diagram for optical reflection

Figure 3.4: Diagram of atomic force microscope (AFM)

Figure 3.5: Intermolecular force curve

Figure 3.6: XRD pattern of ZnO annealed at 600^0C

Figure 3.7: XRD pattern of ZnO annealed at 550^0C
Figure 3.8: XRD pattern of ZnO annealed at 500^0C
Figure 3.9: XRD pattern of ZnO annealed at 450^0C
Figure 4.0: XRD pattern of ZnO thin film as grown sample
Figure 4.1: UV/VIS spectra of ZnO thin film at 500^0C
Figure 4.2: UV/VIS spectra of ZnO thin film at 600^0C
Figure 4.3: Comparison of UV/VIS spectra of ZnO thin film at both the temperatures
Figure 4.4: 3D AFM image of ZnO thin film annealed at different temperatures viz 450^0C, 500^0C, 550^0C and 600^0C
Figure 4.5(a): Force analysis at 600^0C
Figure 4.5(b): Force analysis at 600^0C
Figure 4.5(c): Force analysis at 600^0C

List of Tables:

Table 1: Characteristics of thin films
Table 2: Comparison of thin film deposition parameters by different techniques
Table 3: ZnO thin film on glass substrate (as grown) annealed at different temperatures in O_2 environment
Table 4: Grain Size of ZnO thin film Measured by AFM image analysis at different annealing temperatures
Table 5: Surface Roughness of ZnO thin film measured by AFM at different annealing temperatures

Chapter -1

Thin Film: An Overview

1.1 Introduction

Thin films are layers of a material whose thickness ranges from fractions of a nanometre to several micrometers. They are deposited on the substrates to achieve better properties than that of bulk materials. Electronic semiconductor devices and optical coatings are the main applications benefiting from this technology. Some work is being done with ferromagnetic thin films as well for use as computer memory.

Ceramic thin films are also in wide use. Thin films of ceramic materials like $BaTiO_3$, ZnO etc. has the huge applications in piezoelectric sensors. Coating of ceramic materials protect against corrosion, oxidation and wear.

The nano-structured thin film enhances the efficiency of solar cells, memory storage capacity of computers, reduces the costs of devices as well as material losses. However, thin films have had to be developed using new semiconductor materials, including amorphous silicon, copper indium diselenide, cadmium telluride, zinc sulphide, zinc oxide and film crystalline silicon.

The pivotal role of thin film technology in the development of such diverse and challenging frontiers as microelectronics, optical coatings and integrated optics, thin-film superconductivity and quantum engineering, surface science, engineering and technology, micro-magnetism, metallurgical coatings, and amorphous materials now a part of literature **[1]**. Deposition of thin films increases the contact area of the cell components, resulting in a high fraction of reactants. Thin films result in higher current densities and cell efficiencies because the transport of ions is easier and faster through thin-film layers than in bulk materials [Carolyn Krause].

Transparent and highly conducting oxide films have attracted many researchers due to their wide range of applications in industry as well in research; Transparent and

conducting layers of some metallic oxides such as Cadmium Oxide, Tin Oxide, and Indium Oxide has known for a long time. The electrical property of ZnO thin film strongly depends on the deposition method, thermal treatment and Oxygen chemisorption. Doped ZnO also show a dependence of electrical properties on the substrate temperature and film thickness **[2].** ZnO is one of the metal oxides, which has been widely used as transparent conductor **[3].**

Various techniques have been used for the deposition of ZnO thin films on the glass. In the present work, I have deposited ZnO thin film by tacking ZnO as in powder form and evaporated and deposited on the substrate and then after annealing in air. Among other techniques, Thermal Evaporation method has the following advantages over the others;

1. homogeneity at molecular level
2. low preparation temperature-save energy
3. high deposition rate and
4. less processing time

1.1.1 Properties of thin films

As we move from bulk to nano-structured thin film, the size affects an important role and the properties of these film changes drastically. Thin films are quasi-two dimensional, defect structures different from bulk and strongly influenced by surface and interface effects. Thin film properties are summarized in the Table-1 with their applications.

Table-1: Characteristics of thin films

Thin-film property category	Typical Applications
Optical	Reflective/antireflective coatings, Interference filters, decoration (color, luster), memory disks (CD, DVDs), Wave guides
Electrical	Insulation, Conduction, Semiconductor Devices, Piezoelectric Drives
Magnetic	Memory Disks
Chemical	Barriers to diffusion or alloying, Protection against oxidation or corrosion, Gas/liquid sensors
Mechanical	Tribological (wear-resistant) coatings, Hardness, Adhesion, Micro-mechanics
Thermal	Barrier Layers, Heat Sinks

1.1.2 Thin film growth Process

The growth phenomena in thin films take place in following ways;

Adsorption processes

Adsorption is the process that occurs, when gas or liquid solute accumulates on the adsorbate forming a thin film of atoms or molecules. The adsorption processes are of two types; a) chemisorptions (b) physisorption

The physisorption and chemisorption are distinguished on the basis of their relative bond strength and mechanism. Chemisorption is the process in which chemical bond is formed between the absorbate atom and the substrate. In this case, the adsorption energy Ea ≥ sublimation energy of the substrate (few eV/atom). Physisorption is a type of adsorption in which adsorption adheres to the surface only through Van-der-Waal interections. Physisorption is characterized by low temperature, less than the critical temperature of adsorbate, low enthalpy, adsorption takes place in multi-layers, low activation energy and reversible process. Physisorption energies are of order100 MeV/atom [4].

Condensation

Condensation is the process of accumulation of gaseous particles or atoms by lowering of their energies on the surface for the adsorption process on the substrate.

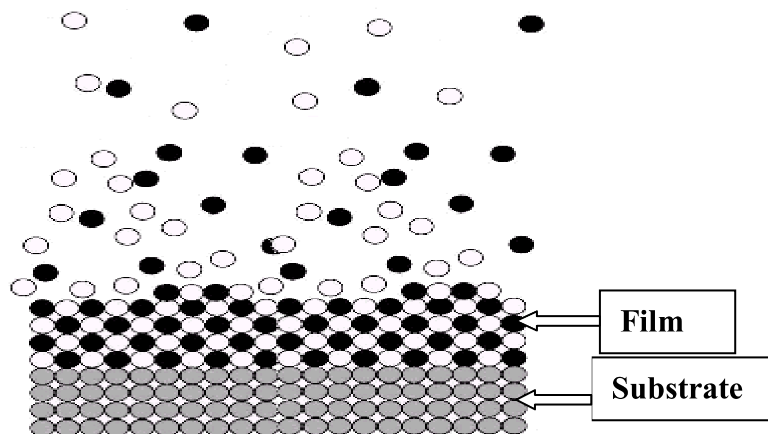

Figure-1.1: Thin film growth process (condensation)

At certain temperature, there is an equilibrium vapour pressure (sublimation pressure); no deposit would occur at all unless one has super-saturation. Super-saturation is achieved

just above the substrate surface. Under super-saturation, the density is so high, i.e. the atomic separation is so short, that condensation occurs due to van der Waals force.

Surface diffusion and nucleation

Surface diffusion

It is the most important factor of thin film structure because it allows the absorbing species to find each other, find most active sites, or find epitaxial sites. Various methods have been applied to measuring surface diffusion rates of absorbed molecules, but most of this work has been done on chemical systems relevant to heterogeneous catalysis rather than to thin film deposition [5]. The role of surface diffusion in thin films has mainly been inferred from observations of thin film structure. Under super-saturation the atoms/molecules are condensed onto the substrate surface. The deposition rate or flux (of adatom) is directly proportional to the pressure and inversely proportional to squire root of absolute temperature. After the atoms being absorbed on the surface, they become adatoms with (positive) adsorption energy E_a, relative to zero in the vapour. The desorption rate of adatom given by,

$$\mathbf{R_a \propto \nu_a \exp(-E_a / kT)} \ \ldots\ldots\ldots\ldots\ldots\ldots\ldots (1.1)$$

Where, ν_a is the characteristic atomic vibration frequency and is expected to vary relatively slowly with T.

The adatom can diffuse over the surface, with energy E_d (migration barrier energy) and the corresponding frequency ν_d (order of 10^{14} / sec). Since $E_d << \boldsymbol{E_a}$, surface diffusion is far more than desorption. The probability that during one second the adatom will have enough thermal energy to pass over the barrier is,

$$\mathbf{P_a = \nu_a \exp(-E_a / kT)} \ \ldots\ldots\ldots\ldots\ldots\ldots (1.2)$$

In unit time, adatom makes ν_d attempts to pass the barrier, with a probability of $exp-(E_d / kT)$ of surmounting the barrier on each try. This is in fact the mean square displacement of the random walker per unit time, or the tracer diffusion coefficient.

Nucleation and growth of 2D islands

The nucleation is the beginning of phase transformation that is formed from gaseous state to solid thin film. Nucleation may involve; the assembly of proper kind of atoms by diffusion, structural change in to one or more intermediate structures, formation of critical sized particles of new phase known as nuclei. Nucleations are two types;

1. homogeneous or self-nucleation
2. heterogeneous nucleation

In the deposition process, the atoms from the gaseous phase settle down on the surface of the substrate and the small nuclei will form at some locations on the substrate. When the density of stable nuclei has increased sufficiently, any further deposition will exclusively lead to island growth. At this saturation island density, the mean free path of diffusing adatoms is equal to the mean island separation and adatoms will attach themselves with much higher probability to existing islands than to create new ones. Approaching coverage of about half a monolayer, islands eventually coalesce which decreases their density. The islands formation is shown in Fig.1.2.

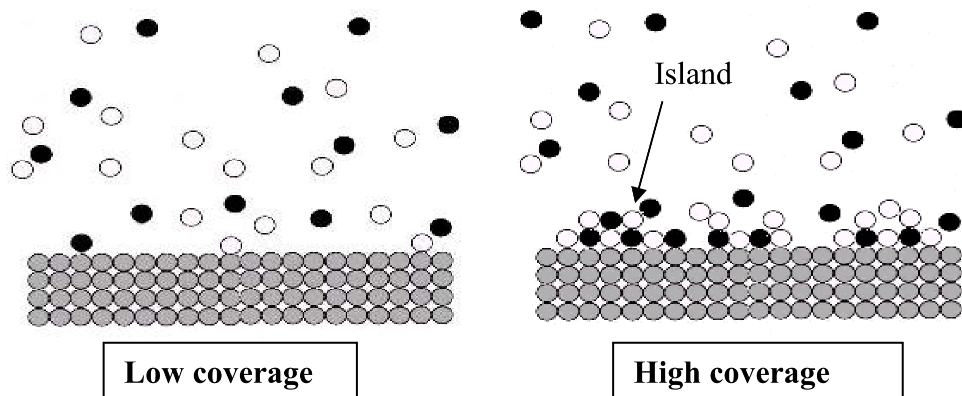

Figure-1.2: Monolayer and Island growth process

If the deposition continues, the nucleation centers become enlarged and formation of 2D islands occurs. The size of the 2D island increases and the coverage of the substrate surface gets enlarged. This process may lead to growth phenomena. The growth fallows the nucleation which determines the final crystallographic structures of the thin films. The thin film growth phenomena are explained in the Fig.1.3.

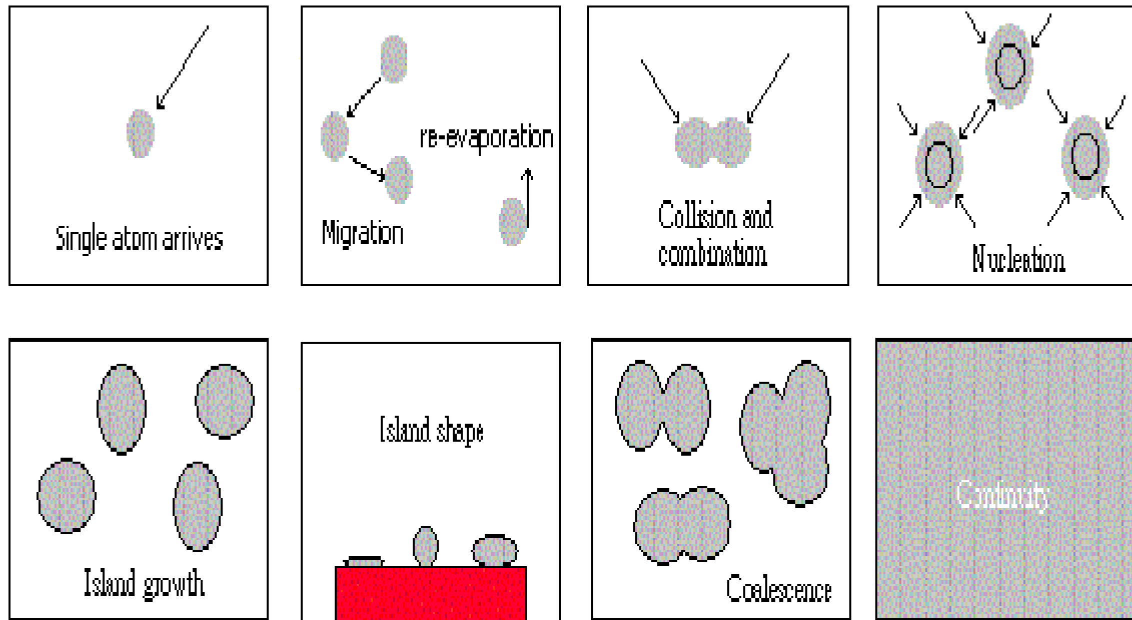

Figure-1.3: Various steps in thin film growth process

Crystallization and film growth

There are mainly three types of structures are obtained in the thin film growth processes.

Amorphous

Structure obtained in this type has no order in the atoms on the layers or structures of the thin films.

Polycrystalline

In this category the randomly oriented grains, oriented grains, highly oriented grains, epitaxy (homo- or hetero-) has been formed.

Single crystal

Single crystal growth process is of two types; homoepitaxy, and hetero-epitaxy. Thin films grown are amorphous as well as crystalline and well understood as in the Fig1.4.

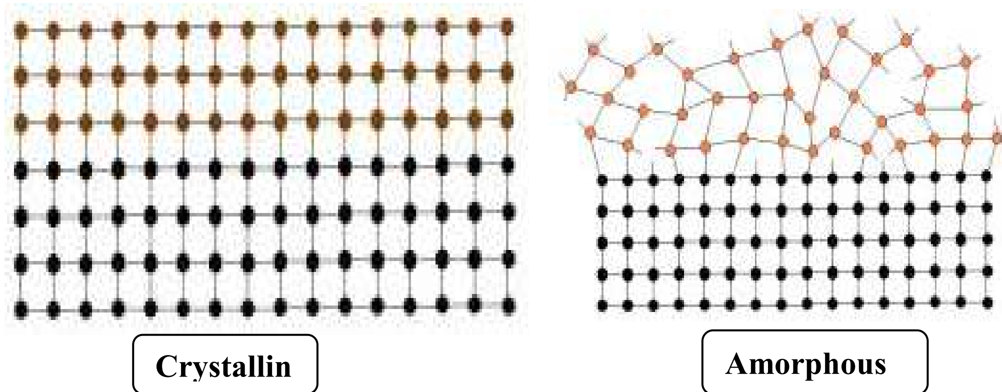

Figure-1.4: Crystalline and amorphous structures of thin film

1.1.3 Epitaxy

Epitaxy is the method of depositing a mono-crystalline thin film onto mono-crystalline substrates. The epitaxy is further classified as in two categories; Homoepitaxy- thin film deposited on the substrate of same materials as that of thin film, and hetero-epitaxy- crystalline thin film grown on the crystalline substrate of different materials.

Factors governing epitaxy

Epitaxy depends on the following factors [4-5],

1. Substrate: Structural compatibility between substrate and the thin film materials are most important factor for epitaxial growth of thin films. There should be lattice matching (crystal structure and lattice constant) between the substrate and the thin film.

2. Chemical compatibility

Chemical compatibility is also required factor for the epitaxial growth of thin films.

3. Temperature

Temperature is also governing factor for epitaxial growth of thin films. The thermal expansion coefficient should be matched. At the elevated substrate temperature Te good epitaxy is obtained. Te depends on the deposition rate, particle energy and the surface contamination. The reason for the need of higher temperature is the reduction surface contamination by desorption, the enhancement of surface mobility of atoms to reach the favorable sites, and the enhancement of diffusivity in the deposit thus favoring re-

crystallization and defect annihilation. The influence of substrate temperature with the film morphology has been shown in the Fig. 1.5.

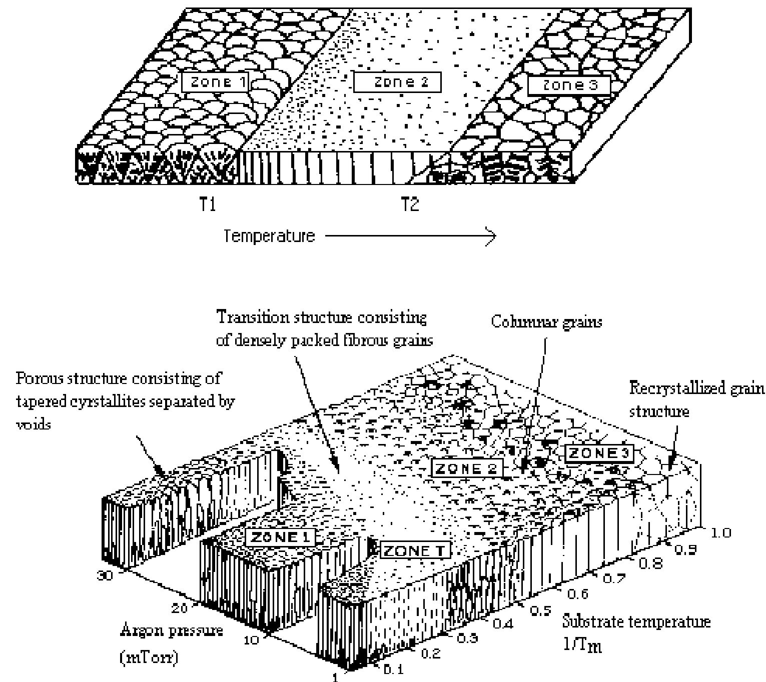

Figure-1.5: Influence of substrate temperature

The classification of three growth modes was first introduced by Ernst Bauer in 1958. These are;

1. **Layer by-Layer, or Frank-Van-der Merwe;** growth mode arises because the atoms of the deposit material are more strongly attracted to the substrate than they are to themselves.
2. **Island (3D), or Volmer-Weber mode;** results in which deposited atoms are more strongly bound to each other than they are to the substrate.
3. **Layer-plus-Island, or Stranski-Krastanov growth mode;** In this case, layers form first, but then for some reason or other the system gets tired of this, and switches to islands.

1.2 Method used for deposition of thin film

Several methods are reported in literature by researchers in order to deposited thin film of different materials by controlling the important parameters and usage of various techniques. These methods are mainly divided into three main category a) physical

vapour deposition, b) chemical vapour deposition and c) chemical solution deposition. Most of the semiconductor devices are grown based on thermal evaporation. We too have used this technique. Fig. 1.6 shows some commonly used techniques for fabrication of thin films.

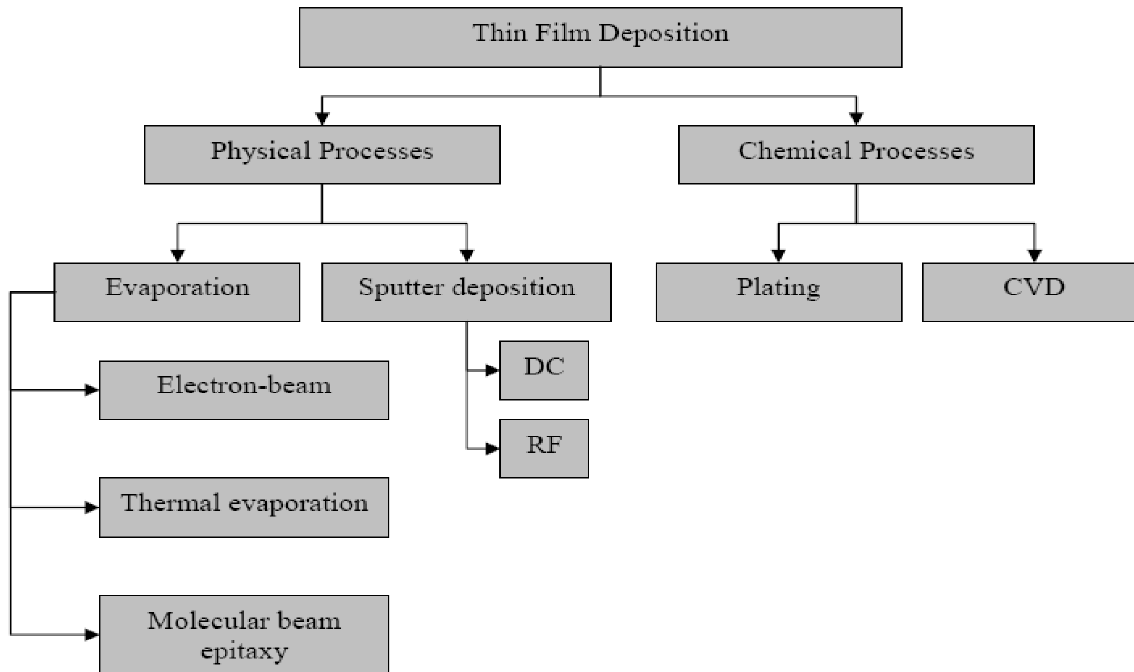

Figure 1.6: Schematic representation of the classification of some of the common thin film deposition processes.

1.2.1 Physical vapour deposition (PVD)

Physical vapor deposition processes are versatile technique used to deposit almost all materials. These processes demonstrate high deposition rates, simplicity and it is relatively easy to use. A wide variety of materials can be deposited, i.e., conductor materials for electronic circuits and devices, for the application of dielectric and optical coatings, and for developing technologies, such as high temperature superconductors.

Physical vapour deposition process, involves the formation of thin films on a substrate by physically depositing the atoms, ions, or molecules of materials. Physical deposition uses mechanical or thermodynamic means to produce a thin film of solid. The material to be

deposited is placed in an energetic, entropic environment (i.e. at high vacuum), so that particles escape its surface and then get deposited on the substrate. The whole system is kept in vacuum deposition chamber, to allow the particles to travel as freely as possible. Physical vapor deposition can be classified as:

1) Thermal evaporation, has following components as heating source; Filament, Resistance Boat, Electron Beam and, Arc Source
2) Sputtering,
   - ✓ RF Sputtering,
   - ✓ DC Sputtering,
   - ✓ Cathodic Arc Plasma Sputtering,
   - ✓ Magnetron Sputtering,
   - ✓ Reactive Sputtering
3) Ion Plating-Reactive Ion Plating
4) Molecular Beam Epitaxy (MBE),
5) Laser sputtering,
6) Cluster-Beam.

Thermal evaporation

The thermal evaporation deposition technique consists in resistive heating of materials, which evaporates in the form of vapor and deposited on to the substrate. A thermal evaporator uses an electric resistance heater to melt the material and raise its vapour pressure to useful range. Low pressures are used, about 10^{-6} or 10^{-5} Torr, to avoid reaction between the vapor and atmosphere. At these low pressures, the mean free path of vapor atoms is the same order as the vacuum chamber dimensions, so these particles travel in straight lines from the evaporation source towards the substrate. Only materials with a much higher vapor pressure than the heating element can be deposited without contamination of the film. The equipments available in the laboratory use resistance heating (Joule effect). The metals used as heating resistance (Boat) are tantalum (Ta), Molybdenum (Mo) and wolfram (W) etc. A schematic diagram of the deposition equipment used in the laboratory is showed in the Fig. **3.1**. Molecular beam epitaxy is a particular sophisticated form of thermal evaporation.

Electron beam evaporator

The technique is based on the heat produced by high-energy electron beam bombardment on the material and material gets melted and goes into vapor state, which is to be deposited on the substrate. The electron beam is generated by an electron gun, which uses the thermionic emission of electron produced by an incandescent filament. Emitted electrons are accelerated towards an anode by a high difference of potential. The crucible itself or a near perforated disc can act as the anode. A magnetic field is often applied to bend the electron trajectory, allowing the electron gun to be positioned below the evaporation line. The Fig. 1.7 shows a diagram of the electron beam gun evaporation equipment.

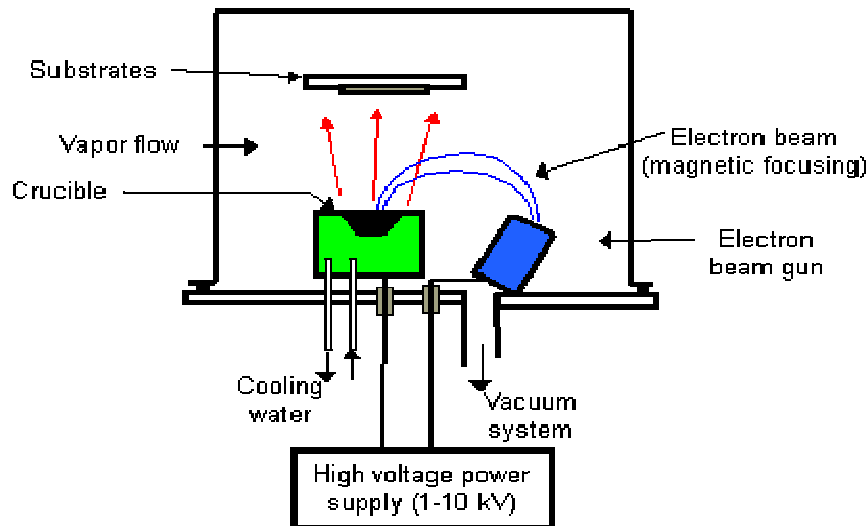

Figure 1.7: Electron beam evaporator

Sputtering

Sputtering is the process of ejection of atoms from solid target materials due to bombardment of high energetic ions. Sputtering was first observed by Grove in 1852 and Pulkerin 1858 using von Guericke-type oil-sealed piston vacuum pumps. Sputter deposition of films was first reported by Wright in 1877. It is useful for compounds or

mixtures, where different components would otherwise tend to evaporate at different rates. The schmatic of sputtering process is shown in the Fig.1.8.

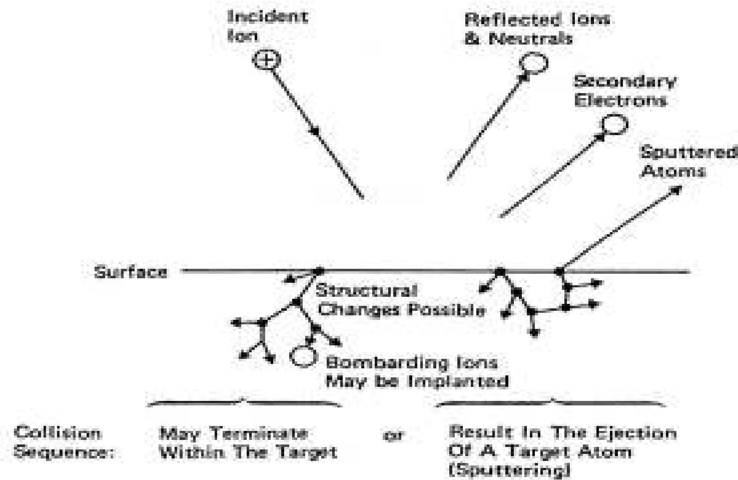

Figure 1.8: The schematic representation of the fundamental processes occurring during sputtering

Magnetron sputter deposition

The prototype of the first magnetron was a mercury electrode lamp, first used by Kisayevand Pashkovain 1959 and adapted in a flat form by J.S. Chapin in 1974 to deposit thin films. Magnetron sputtering is one of the most broadly used techniques mainly on account of the high rate of target sputtering and the reduced range of operating pressures. The constant magnetic field generated by magnets serves to localize the glow discharge on the surface of the water-cooled sputtered targets, leading to much higher ionization efficiency, and denser plasma formed near the cathode at low pressures.

Pulsed laser deposition

Pulsed laser deposition (PLD) system works by an ablation process. Pulses of focused laser light vaporize the surface of the target material and convert it to plasma; this plasma usually reverts to a gas before it reaches the substrate.

Cathodic arc deposition

Cathodic arc deposition or Arc-PVD which is a kind of iron beam deposition where an electrical arc is created that literally blasts ion from the cathode. The arc has an extremely high power density resulting in a high level ionization (30-100%), multiply charged ions, neutral particles, clusters and macro-particles (droplets).

Molecular beam epitaxy (MBE)

This process is very slow, more costly and gives high quality thin film. This is a sophisticated, finely controlled method for growing single-crystal epitaxial films in a high vacuum of about 10^{-11} torr. The films are formed on single-crystal substrate by slowly evaporating the elemental or molecular constituents of the film from separate Knudsen effusion source cells onto substrates held at a temperature appropriate for chemical reaction, epitaxy, and re-evaporation of excess reactants. The furnaces produce atomic or molecular beams of relatively small diameter, which are directed at the heated substrate, usually silicon or gallium arsenide. Fast shutters are interposed between the sources and the substrates. By controlling the shutters, one can grow super lattices with precisely controlled uniformity, lattice match, composition, dopant concentrations, thicknesses, and interfaces down to the level of atomic layers.

1.2.2 Chemical vapor deposition (CVD)

Chemical vapour deposition is the process of chemically reacting volatile compounds of a material to be deposited, with other gases, to produce a non-volatile solid that deposited atomistically on a suitably placed substrate.

Types of chemical vapor deposition

A number of forms of CVD are in wide use and are frequently referenced in the literature. Classified by operating conditions are as:

1-Atmospheric pressure CVD (CVD)- CVD processes at atmospheric pressure.

2-Low pressure CVD (LPCVD) (at 0.2~20 torr)

Reduced pressure tends to reduce unwanted gas-phase reactions and improve film uniformity across the wafer. Most modern CVD processes are either LPCVD or UHVCVD.

3-Metal organic CVD (MOCVD)

Metalorganic vapour phase epitaxy (MOVPE) is a chemical vapour deposition method of epitaxial growth of materials, especially semiconductors from the pyrolysis of organic compounds containing the required chemical elements.

4-Plasma enhanced CVD (PECVD)

PECVD process is that utilize plasma to enhance chemical reaction rates of the precursors. PECVD processing allows deposition at lower temperatures, which is often critical in the manufacture of semiconductors. Plasma is used to force a reaction that would not possible at low temperature.

The table-2 can summarizes the comparison between different techniques for thin film deposition.

Table-2: Comparison of thin film deposition parameters by different techniques

Process	Material	Uniformity	Impurity	Grain Size nm	Film Density	Deposition Rate (A/s)	Substrate Temperature (°C)	Directional	Cost
Thermal Evaporation	Metals or Low melting point materials	Poor	High	10~100	Poor	10~20	50~100	Yes	Very Low
E-beam Evaporation	Both metal and Dielectrics	Poor	Low	10~100	Poor	10~100	50~100	Yes	High
Sputtering	Both metal and Dielectrics	Very Good	Low	~10	Good	For Metal: ~100 For Dielectric: ~1-10	~200	Some Degree	High
PECVD	Mainly Dielectrics	Good	Very Low	10~100	Good	10~100	200-300	Some Degree	Very High
LPCVD	Mainly Dielectrics	Very Good	Very Low	1~10	Excellent	10~100	600~1200	Some Degree	Very High

1.2.3 Chemical solution deposition (CSD)

Chemical root is the bottom up approach; hence this method gives better control over size and shape of the film. In chemical solution deposition method, there is no requirement of vacuum and hence this method is cheap and simple to handle.

Based on literatures CSD are of mainly three types as follows;

1- Photo-chemical Deposition (PCD)
2-Chemical Bath Deposition (CBD)
3- Sol-Gel processing--- Spin Coating, dip or immersion coatings.

Photochemical deposition method

A photochemical solution deposition method comprises introducing a starting chemical solution into a reaction chamber, irradiating the starting chemical solution and substrate surface with a light energy, and forming a deposition film on a substrate by utilizing a photochemical reaction, characterized in that the plural starting chemical solutions are introduced into the reaction chamber and the film is formed on said substrate by causing chemical reactions by irradiating molecules of these starting solution with individual light energy having a wavelength region corresponding to an absorption spectrum of each of said starting solution.

Chemical bath deposition (CBD)

The most used solution technique and also one of the oldest methods for thin film growth is chemical bath deposition (CBD) or chemical solution deposition (CSD). CBD has been widely used for the deposition of chalcogenides for various applications. In CBD all the precursor ions are present at the same time in the reaction vessel. Typically CBD has a so-called terminal thickness indicating a point where the growth of thin film is stopped due to depletion of precursors in the solution. The precursor molecules are metastable releasing slowly ions for the deposition reaction. The product has low solubility, but due to limited number of free ions a direct homogeneous precipitation in the solution is prevented.

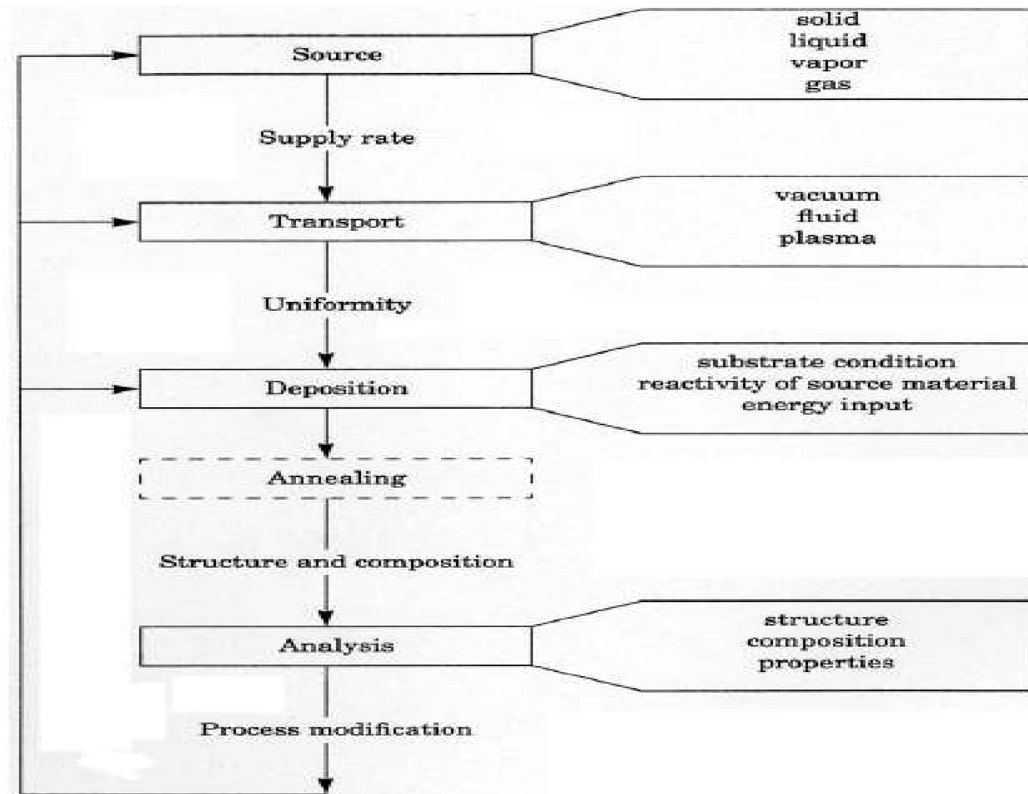

Figure-1.9: Thin film deposition steps

For metal sources complexed ions are usually utilized. Generally sulphur and selenium sources are decomposable molecules, like thiourea or thioacetamide and selenourea, respectively[6-8].

Sol-gel coating

Sol-gel processing is widely used in the synthesis of inorganic and organic-inorganic hybrid materials and capable of producing nanoparticles, nanorods, thin films, and monolith. Sol-gel methods for oxide coatings were reviewed by Francis. Prior to sol-gel transition or gelation, sol is a highly diluted suspension of nanoclusters in a solvent, and typically sol-gel films are made by coating sols onto substrates. Most commonly used methods for sol-gel film deposition are spin- and dip-coatings, though spray and ultrasonically pulverized spray were also used.

In dip coating, a substrate is immersed in a solution and withdrawn at a constant speed. As the substrate is withdrawn upward, a layer of solution is entrained, and a combination of viscous drag and gravitational forces determines the film thickness, H:

$$\mathbf{H = c_1(\eta U_o/\rho g)^{1/2}} \qquad \text{(1.3)}$$

Where η is the viscosity, U_o the withdrawal speed, ρ the density of the coating sol, and $\mathbf{c_1}$ is a constant. Fig. 2.0 illustrates various stages of the dip-coating process.

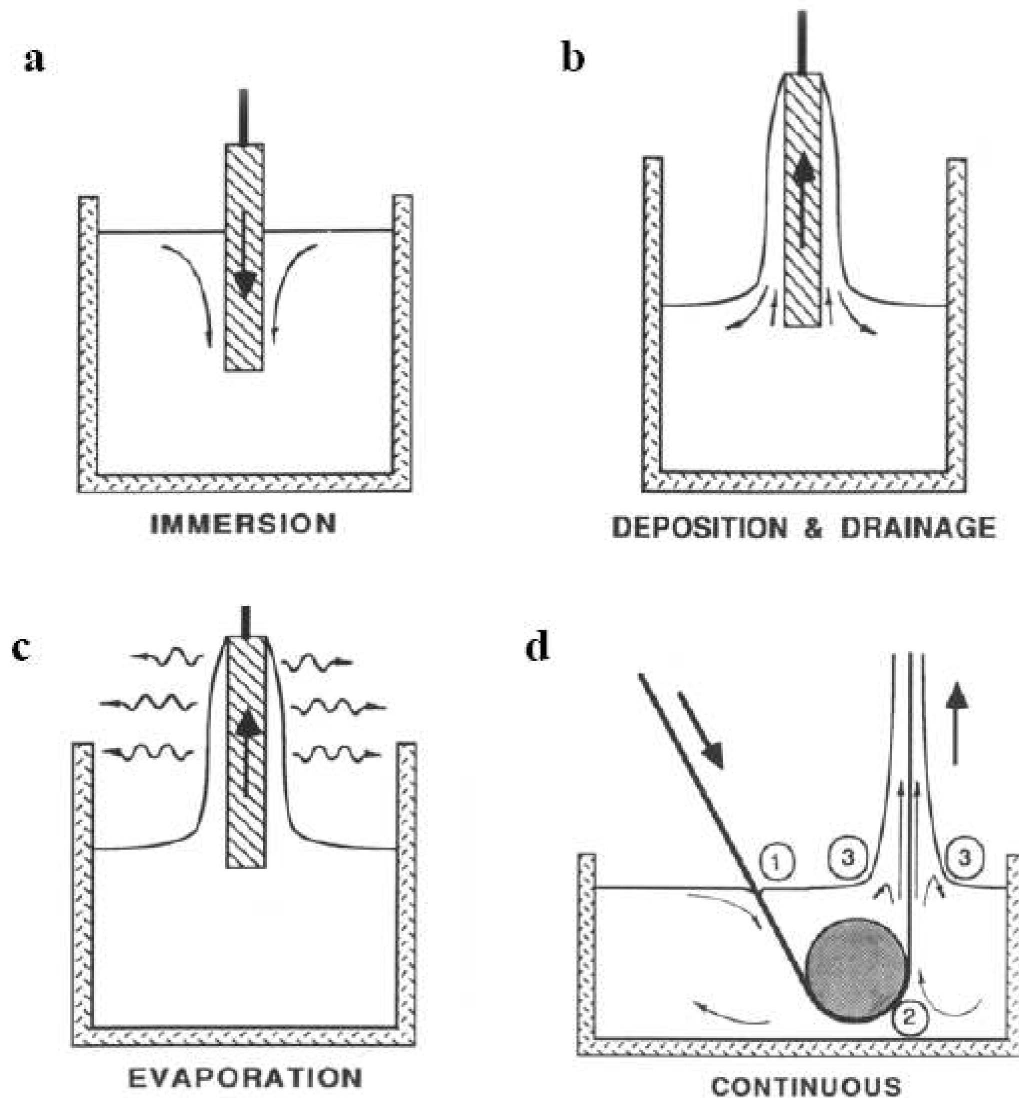

Figure-2.0: Various stages of dip coating process

It should be noted that the equation does not account the evaporation of solvent and continuous condensation between nanoclusters dispersed in the sol as illustrated in Fig. 2.1.

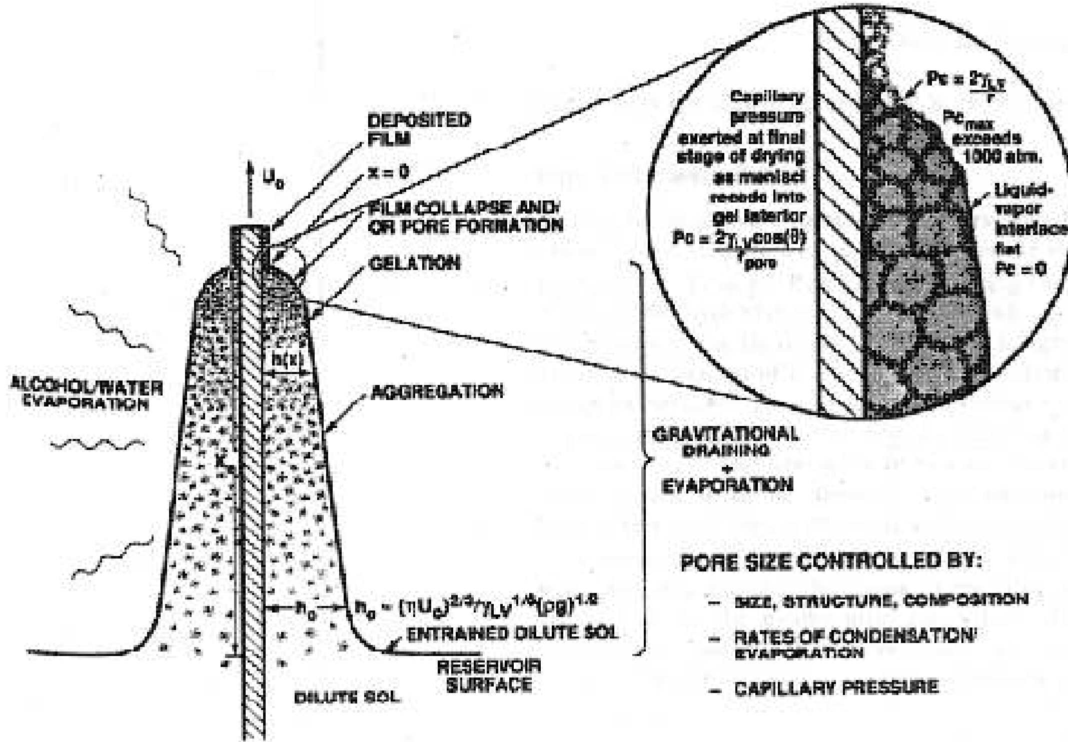

Figure-2.1: Sol-gel dip-coating processes

However, the relationship between the thickness and the coating variables is the same and supported by the experimental results, but the proportionality constant is different. The thickness of a dip-coated film is commonly in the range of 50-500 nm, though a thinner film of ~ 8 nm per coating was also reported [9].

1.3 ZnO the novel material

Most of the literatures reveal that the thin film technologies are also being developed as a means of substantially reducing the cost of photovoltaic systems, electronic equipments and enhance the device performance. The nanostructured thin film enhances the efficiency of solar cells, memory storage capacity of the computers, reduces the costs of the devices as well as the materials losses. Transparent conducting films continue to receive considerable attention from both fundamental and application point of view primarily because of their useful properties [2].

The thin films of ZnO generated immense interests as a transparent semiconducting materials, because of coating of this material are relatively inexpensive and have sharp UV cut-off, that is why they are used as heterojunction solar cells based on CdTe, $CuInSe_2$ [10-11] and CuInS [12]. ZnO is also used for piezoelectric devices such as surface acoustic wave (SAW) devices [13]. Among the transparent conducting oxides, ZnO is probably the most commonly studied material as it has the following unique merits. First, ZnO is a wide band gap semiconductor that has huge potential for electronic, opto-electronic, and optical applications. Second, it is unique in having semiconducting, piezoelectric, and pyro-electric properties, and is an ideal candidate for fabricating electromechanical coupled devices [14]. Third, ZnO is a biodegradable and possibly biocompatible material suitable for medical and biological applications [15].

Various techniques have been used for deposition of ZnO thin film namely, Pulsed Laser Deposition [16-17], Atomic Layer Deposition [18], Spray Pyrolysis [19,20-21], Metal Organic Chemical Vapor Deposition [22-23], DC Magnetran Sputtering [24], Photo Induced MOCVD [16], Reactive Molecular Beam Epitaxy [25], Molecular Beam Epitaxy [26]. The Zinc Oxide film deposited from the above techniques has both low resistivities and high transparency in the visible region. There are merits and demerits for each deposition technique, for example sputtering techniques allow the fabrication of high quality films but the equipment cost is very high with a low production rate. At the same time spray techniques are very cheap but the films produced are not consistent. There is a lot of variation in the results reported by different workers using different techniques. The

variation is due to the difference in the deposition parameters and the purity of the elements. Literatures show that variation in the process parameters give the many more nano-structures and different morphology by the thermal evaporation technique and we can control these parameters easily. The thermal evaporation system method is less costly than other methods for depositing the ZnO nano-structured thin films. Semiconductor nano-wires are a promising candidate for fabrication of basic nano-devices and complicated nano-circuits [27, 28-29]. Zinc Oxide is a versatile functional semiconductor with wide applications, such as the gas sensor and the transparent conducting film in the flat display screen [30]. The outstanding features of zinc oxide with a wide band gap (3.37eV) and a large excitonic binding energy (60 meV) lead to the existence, extremely stability, of exciton at room temperature, and enable ultraviolet luminescence (UV) lasing in ZnO crystals. The ultraviolet luminescence from nanophase ZnO crystals in the form of thin film or particles has been widely studied in recent years [31, 32-33]. By optimizing the process parameters in the thermal evaporation system we can make ZnO nano-dots, nano-rods, nano-springs and nano-belts. Literatures show that Nano-rods and nano-belts of ZnO have tremendous applications in the sensors and memory applications at nano scales. By the review of lots of literature survey, our attention goes towards the development of ZnO nano-structures by the thermal evaporation technique.

Chapter -2

Synthesis and Experimental Techniques

2.1 Design of experimental set-up

In order to deposit thin film of ZnO on glass substrate, we have designed and fabricated an indigenous thermal evaporator to achieve relatively high vacuum to improve the quality of thin film.

The system assembly contains the following;

- ✓ Rotary pump
- ✓ Diffusion pump
- ✓ Resistive heating element.
- ✓ Gauges (Pirani and Penning)
- ✓ Liquid Nitrogen trap, and
- ✓ Thickness monitor,

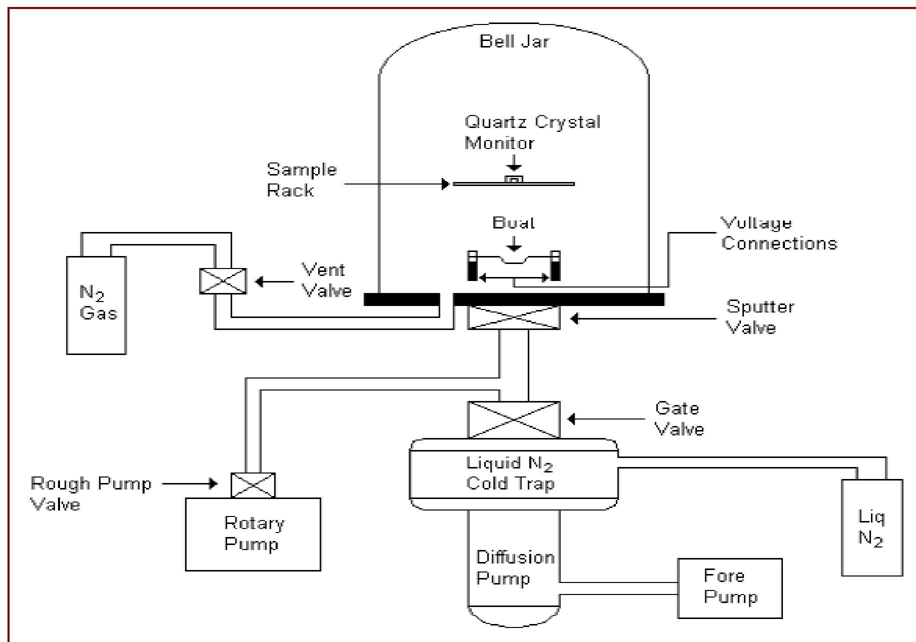

Figure 2.2: Thermal Evaporator System Designed and Fabricated

The systematic design of the thermal evaporator is shown in Fig. 2.2. All the parts taken from the other instruments like E-beam evaporation system and old model of thermal evaporator, which are dismantled, and not in use. The diffusion pump and rotary pump

are taken from these instruments. All the necessary parts have been designed in lab and fabricated in the Workshop.

2.1.1 Fabrication of coupling arrangement of turbo pump to vacuum chamber:

The most time consuming job was to design and fabrication of the coupling arrangement of the diffusion pump with the liquid nitrogen trap and diffusion pump to the vacuum chamber. The completed coupling arrangement is shown in the figure and images.
We can see all the components, which connect the vacuum chamber base to the pump head below.

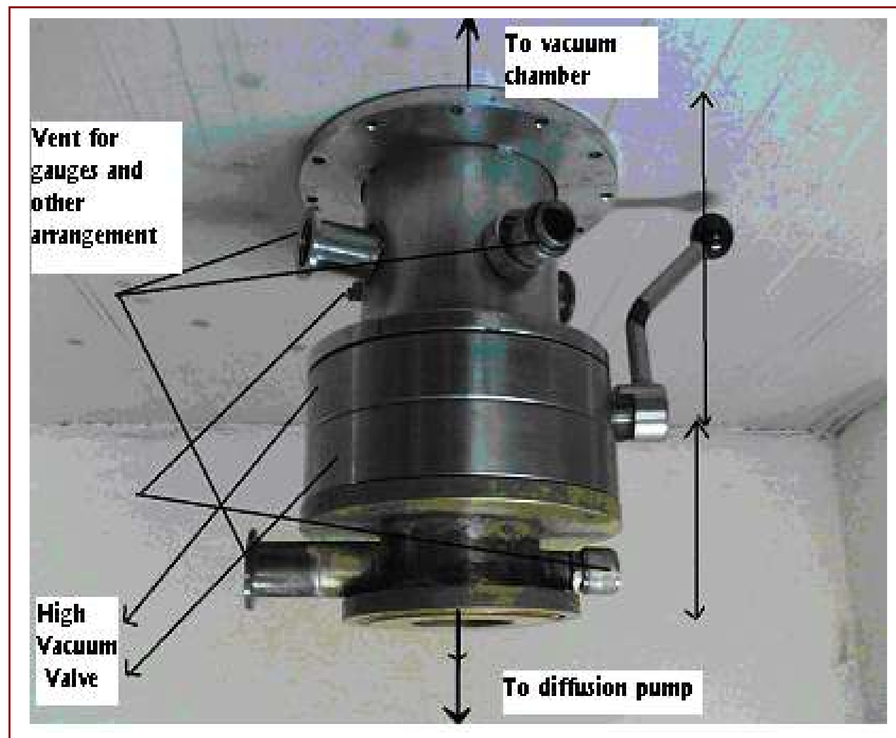

Figure 2.3: Coupling arrangement with high vacuum valve

The first part of the assembly which connects the chamber base with the butterfly valve is shown below, which a stainless steel pipe is having two flanges on two ends of it. This pipe also has two-gauge head inlet and an air admittance inlet. This part was taken from some old set up of the lab.

Figure 2.4: Butterfly valve

Figure 2.5: Ring for rotation of valve

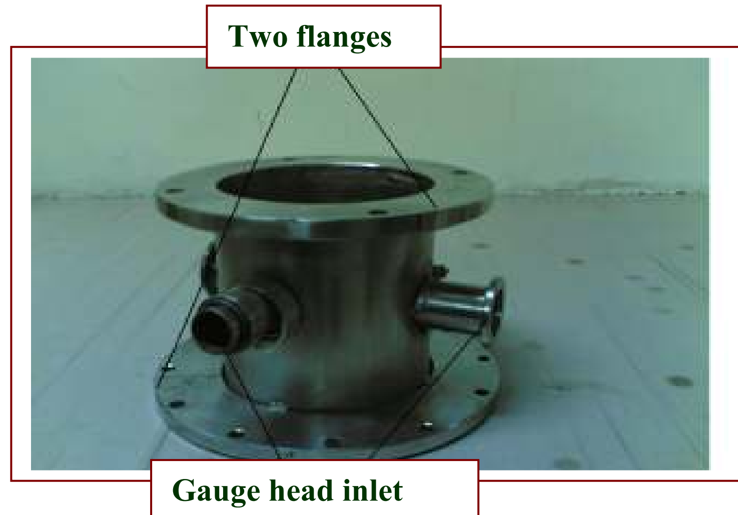

Figure 2.6: Flanges with gauge head inlets

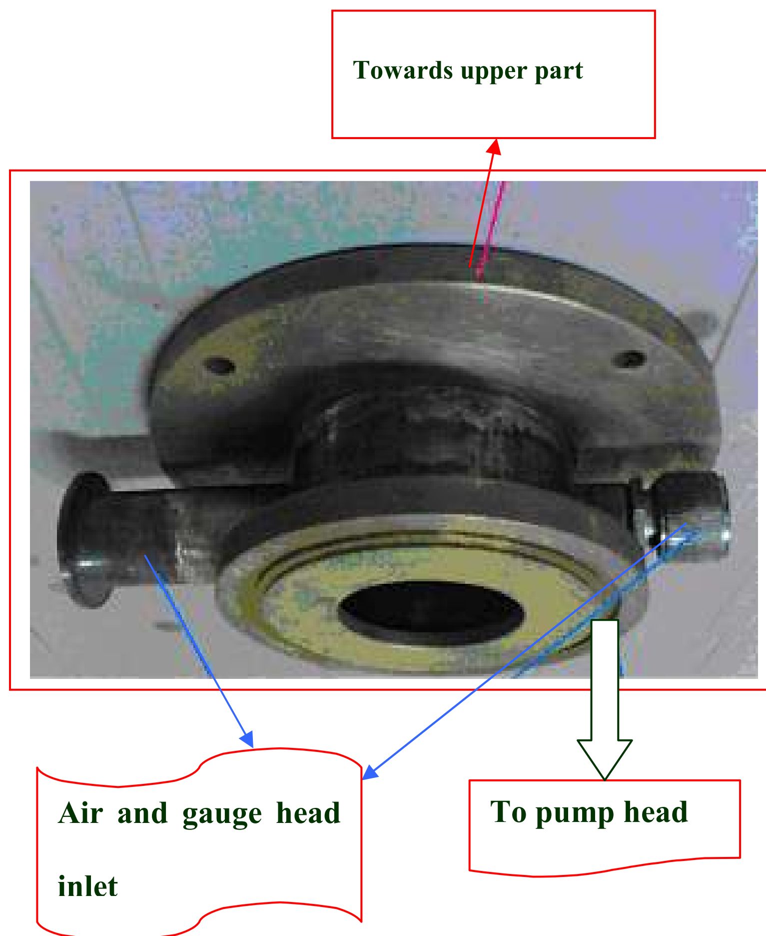

Figure 2.7: Flanges, which joins the pump

2.1.2 Fabrication of resistive heating arrangement of the material to be deposited:

Arrangement is made as usual .It is shown in the image below. I have used arrangement of two copper strips to pass current through the tungsten boat in which the material is kept for deposition.

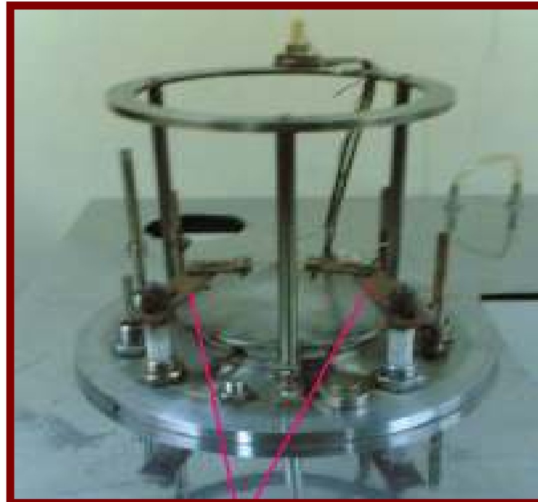

Figure 2.8: Resistive heating and other components arrangements

Thus the vacuum chamber is coupled with the Diffusion pump and with the Rotary pump by these couplings. Each and every part of the set up is now ready, just the assembling of the all parts has to be done.

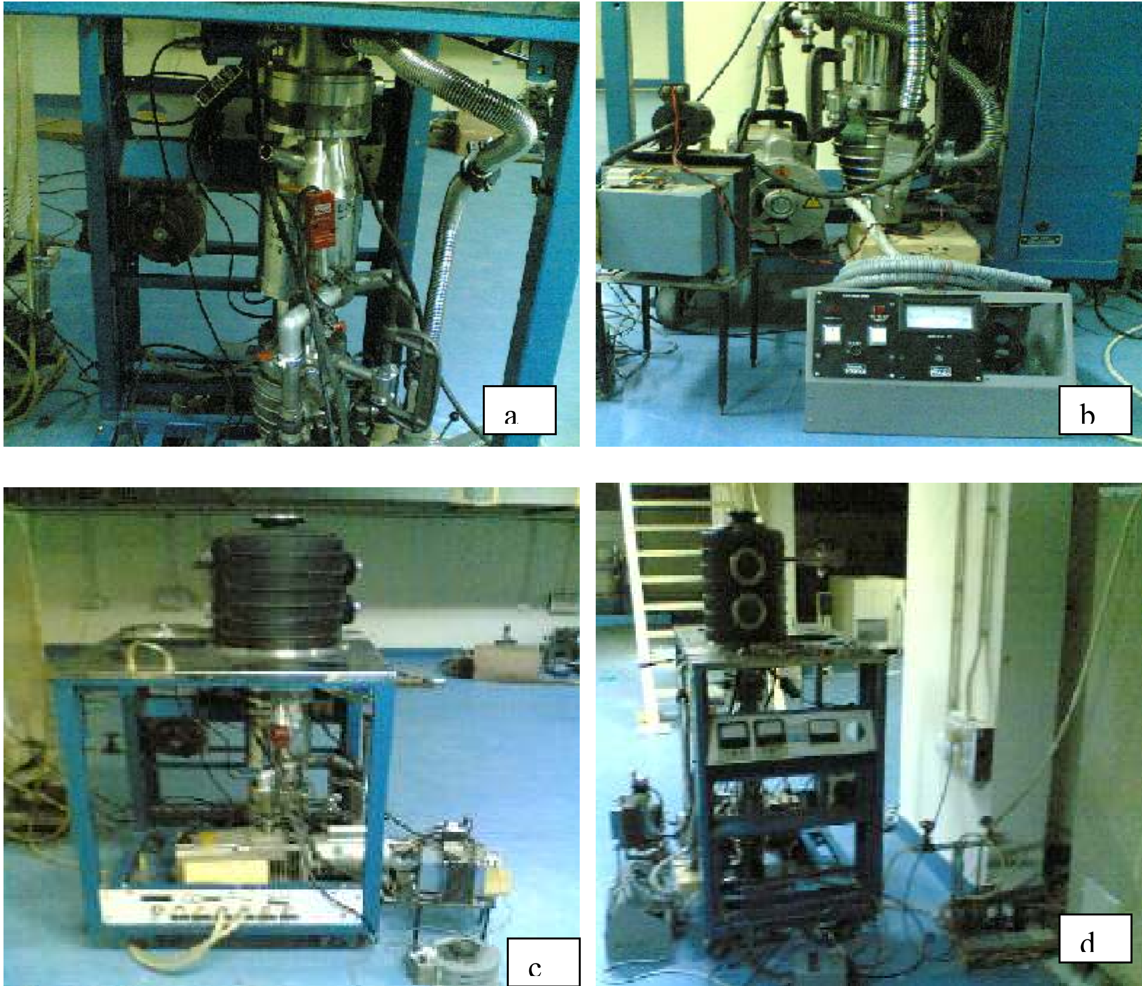

Figure 2.9: Thermal Evaporator fabricated at central nuclear lab IIT Kanpur

After getting different part assembled the testing of vacuum is to be done many times. All the times we get vacuum range up to 10^{-6} mbar. Now the thermal evaporator system is to be ready for the deposition of material like gold, silver and compounds on the suitable substrates.

2.2 Deposition of thin film

2.2.1 Experimental set-up used for ZnO thin film deposition

2.1.2 Materials used

ZnO has received much attention over the past few years because it has a wide range of properties that depends on doping, including a range of conductivity from metallic to insulating (including n-type and p-type conductivity), high transparency, piezoelectricity, wide-band gap semi-conductivity, room-temperature ferromagnetism, and huge magneto-optic and chemical sensing effects. We review recent studies of ZnO nanostructures, fabrication, novel device applications, and its potential as an electron acceptor material in hybrid solar cells. ZnO is found as spintronic materials because it shows ferroelectric behavior even at room temperature [34]**.** We have found in some literatures, ZnO thin film used as nano-cantilevers for AFM tip and sensor applications. Intense research by many different groups has focused on novel nanostructures with different shapes ranging from nanostructured thin films, nanowires to nanobelts and even nanosprings. This makes it interesting as laser material based on exciton recombination at room temperature or even higher**.()** ZnO is a material of wide ranging application [35]. Not only it finds application in various photonic associated technologies, because of its piezoelectric nature, it can be used effectively as a sensor in various MEMS related devices. **(NPL)** ZnO occurs in the nature as the mineral Zincite. Zinc oxide crystallizes in the hexagonal wurtzite structure in which the oxygen atoms are arranged in a hexagonal close-packed type of lattice with zinc atoms occupying half the tetrahedral sites with space group see in the Fig. 3.0.

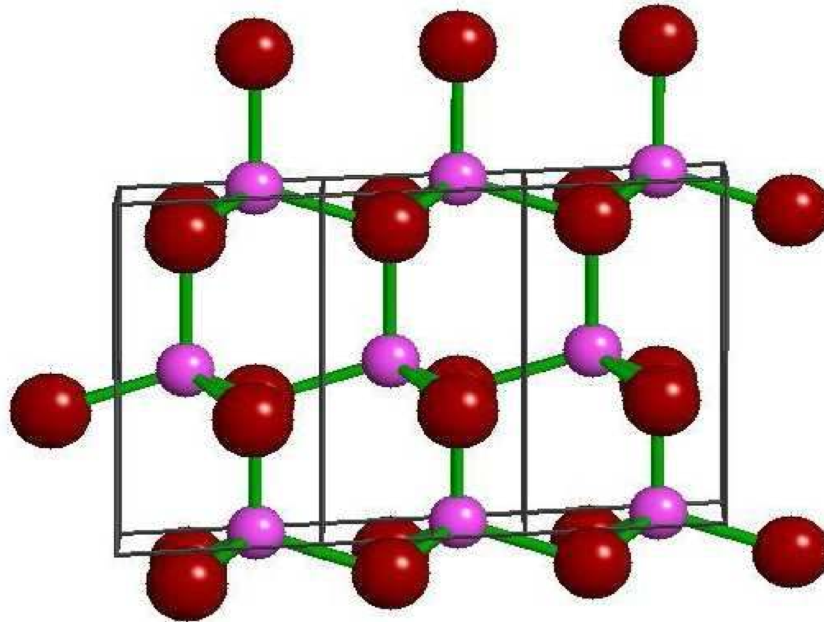

Figure 3.0: The Hexagonal wurtzite crystal structure of ZnO. The larger red atoms are zinc atoms while the smaller purple atoms are oxygen atoms.

We have taken Zinc Oxide powder from MERK AR grade (99.98% purity, as received) as an evaporant for deposition. We have used Mo boat for resistive heating of the sample. For boat selection, we have taken care of different parameters like reactivity, melting point, boiling point and difference in electronegativity of both the boat and evaporant.

Here we have taken glass as the substrate material for depositing thin film of zinc oxide and other chemical reagents like soap solution, trichloroethanol, chromic acid, acetone, ethanol and methanol for cleaning the substrate.

2.2.3 Methodlogy

Following flow chart explains the our methodlogy to deposite and characterize the zinc oxide thin film.

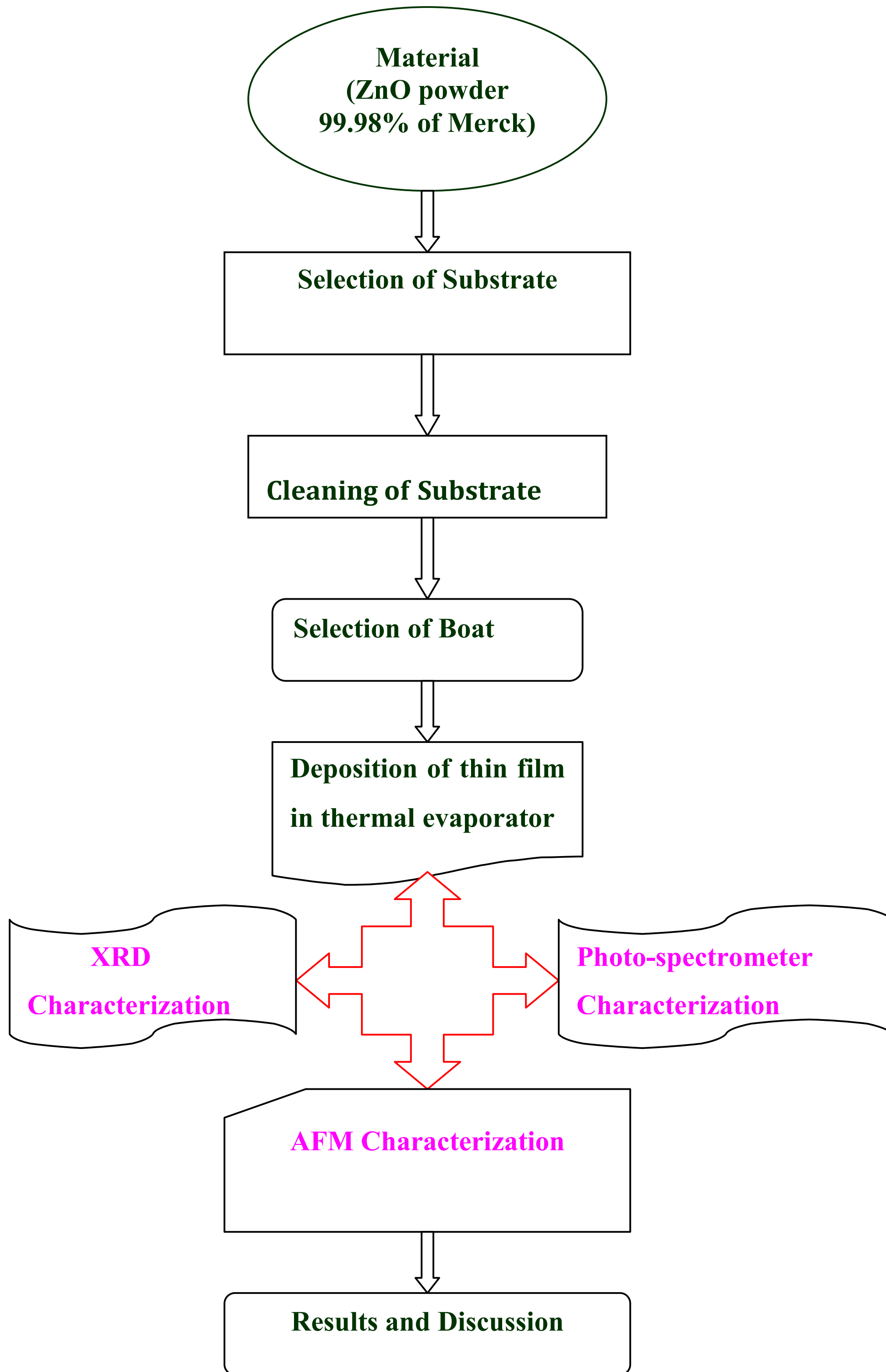
Material
(ZnO powder
99.98% of Merck)
Selection of Substrate
Cleaning of Substrate
Selection of Boat
Deposition of thin film
in thermal evaporator
XRD
Characterization
Photo-spectrometer
Characterization
AFM Characterization
Results and Discussion

2.2.4 Substrate cleaning

A thoroughly cleaned substrate is essential for the preparation of films having good adhesion and reproducible properties. The choice of cleaning procedure depends on the nature of substrate, the type of the contaminants and the degree of cleanliness required. Following flow chart was used for cleaning purpose of glass substrate and Si substrates.

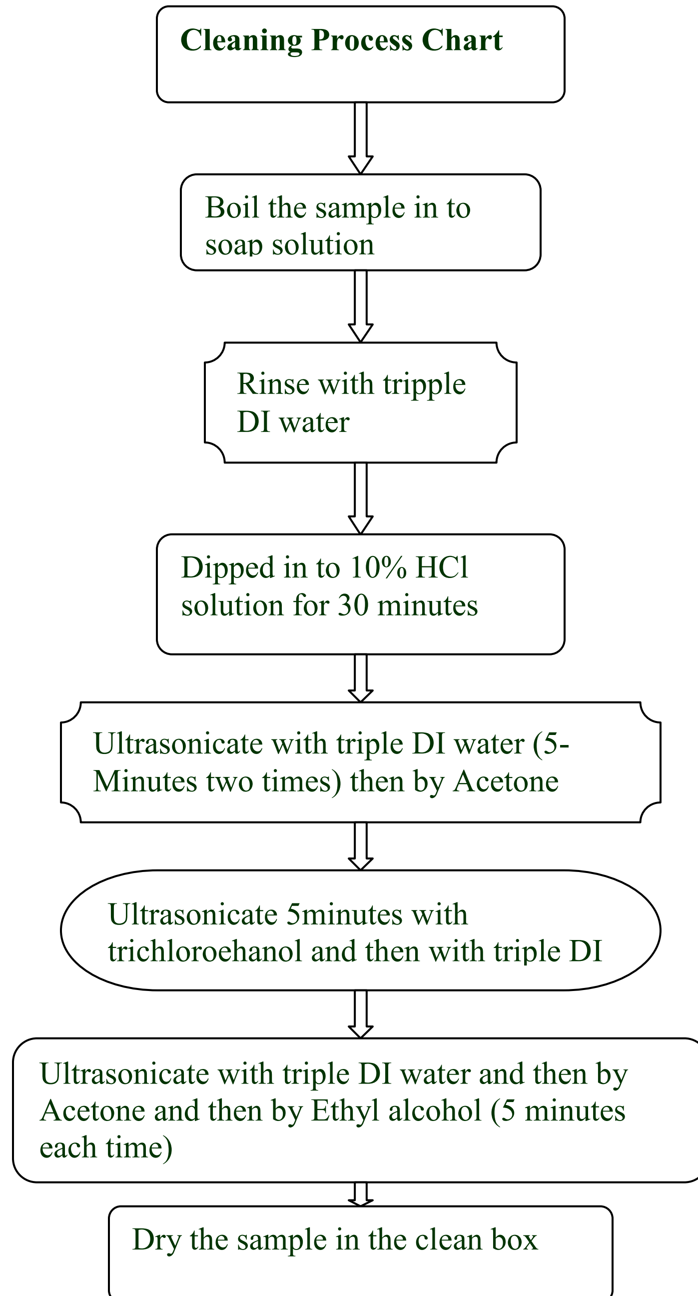

2.2.5 Experimental procedures

ZnO nano-structured thin film is deposited by thermal evaporation, a physical vapor deposition technique. Basically, we are putting ZnO powder on the Mo light boat, and heating it to the point where the ZnO actually evaporates, and then condenses on our (relatively) cold sample surface (as well as elsewhere in the chamber).

Figure 3.1: Thermal evaporator used for deposition

I. Start the system:

1. Turn on the water to the diffusion pump.
2. Turn on the pump station main power and the gauge controller power.
3. Make sure the entire vacuum valves are closed (clockwise closes, counterclockwise opens).
4. Open the mechanical pump vent, turn on the mechanical pump, and then close the vent.
5. Open the Mechanical Pump to Diffusion Pump valve.
6. When the pressure drops below 10^{-3} mtorr, turn on the diffusion pump and let it warm up for 30 minutes.
7. Carefully add liquid nitrogen to the cold trap until it is fully cooled. (It will limit our base pressure).

II. To use the vacuum chamber:

1.Open the chamber vent valve for a couple of minutes; until air no longer can be heard entering the chamber and the bell jar is free from the base plate. Raise the bell jar, and lock it in place.
2. Mount your samples and a glass slide (for thickness monitoring) on the sample holder.
3. Carefully, unlock the bell jar and lower it into place.
4. Close the chamber vent valve, close the Mechanical to Diffusion Pump valve, and open the Mechanical Pump to Bell Jar valve.
5. Roughing the bell jar with the mechanical pump until the Bell Jar pressure is less than 10^{-2} mtorr.
6. Close the Mechanical Pump to Bell Jar valve and then open the Mechanical Pump to Diffusion Pump valve.
7. Open the Diffusion Pump to Bell Jar valve and turn on the Bell Jar ionization gauge. The system should pump down to approximately $10^{-(4-6)}$ mtorr, if the cold trap is fully cooled with liquid nitrogen. This may take 10-20 minutes.
8. Set the filament selector to your desired filament, make sure the filament adjust is set to zero, and turn on the filament power.

9. Increase the filament current slowly by turning up the filament adjusts. Somewhere around 30A the filament should begin to glow. Proceed with the evaporation.

10. When the evaporation is complete, slowly turn down the filament adjusts to zero, and turn off the filament power.

III. Remove sample and pump down

1. Wait about 5 minutes for the filament and chamber region around it to cool off.
2. Close the Diffusion Pump to Bell Jar valve and turn off the Bell Jar ionization gauge.
3. Open the chamber vent valve for a couple of minutes; until air no longer can be heard entering the chamber and the bell jar is free from the base plate. Raise the bell jar, and lock it in place.
4. Remove your sample and the glass slide.
5. Follow the procedure above beginning at step II-3 and ending at step II-7 to put the chamber under high vacuum. If you are going to leave the system in this state for a while, turn off the ionization gauge.
6. Now we can get a calibration by measuring the thickness of the ZnO on the glass slide using the Profilometer and the thickness monitor.

IV. To shut down the system

1. Turn off the Bell Jar ionization gauge (and filament power if it is not off).
2. Close the Diffusion Pump to Bell Jar valve.
3. Turn off the diffusion pump power and let it cools for at least 30 minutes.
4. Close the Mechanical Pump to Diffusion Pump valve.
5. Turn off the mechanical pump power and open the mechanical pump vent.
6. Turn off the diffusion pump cooling water.
7. Turn off the gauge controller power and the pump station main power.

V. Percussion

There are no chemical hazards associated with the vacuum system. The main concerns are maintaining the integrity of the vacuum. Latex gloves should be worn at all times when handling anything on the interior of the vacuum chamber. It is very important to follow the pump down sequence below **EXACTLY** in order not to damage the system (and save you many hours of cleaning up the chamber). In addition, heat and cool the filaments at the rate specified so as not to burn out the heating wire.

2.2.6 Annealing of samples

As deposited thin film has stresses and less crystalline and could not be used for device purpose because stresses reduce the desired properties of the film. A method to reduce the stresses and improves the crystallinity was needed. The first obvious approach was to anneal the sample to try to relax the ZnO film. Adhesion property also improves on annealing the sample. Now we have annealing the sample at different temperatures. We have as grown film appearance brown color that indicates the film has some metallic nature.

Table 3: ZnO thin film on glass substrate (as grown) annealed at different temperatures in O_2 environment

SAMPLE	ANNEALING TIME (IN MINUTES)	ANNEALING TEMPERATURE ºC
A	30	450
B	30	500
C	30	550
D	30	600

2.3 Charcterization techniques

2.3.1 X-ray diffraction

A powerful technique used to uniquely identify the crystalline phases present in materials and to measure the structural properties (strain state, grain size, epitaxy, phase composition, preferred orientation, and defect structure) of these phases; also used to determine the thickness of thin films and multi-layers, and atomic arrangements in amorphous materials (including polymers) and at interfaces. Bragg's Law gives condition for constructive interference from planes with spacing d_{hkl},

$$\lambda = 2d_{hkl} \times \text{Sin}\theta_{hkl} \ldots\ldots\ldots\ldots\ldots\ldots\ldots\ldots\ldots\ldots\ldots\ldots\ldots\ldots(1.4)$$

The X-ray diffraction patterns of various samples of ZnO thin films has been recorded using Ritch-sefert X-ray diffractometer(at IIT Kanpur) (model ISO Deby film 2002) with CuK_{α} radiation of wavelength 1.5418 A^0 and Rigaku model Geiger diffractogram with CuK_{α} radiation (λ = 1.5418 Å) obtained from the copper target using an in built Ni filter (at TCIRD) to acertain crystalinity, and the phases present. For zinc oxide thin film, the film coated on the glass slides was directly tcken held in the mounting on the diffractometer. The X-ray scaning rate was 3^0 per minute.

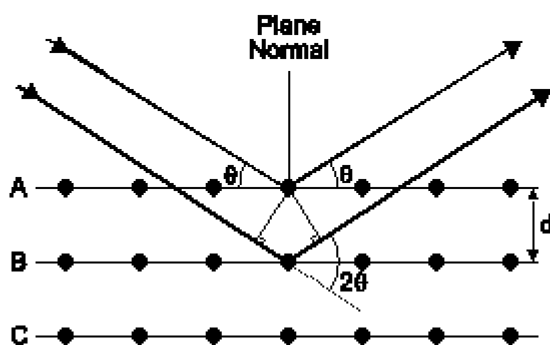

Figure 3.2: X-ray reflection pattern

2.3.2 UV-VIS spectrophotometer

Optical transmittance (T) of ZnO thin film was measured in the wavelength range of 250nm to 500nm with the UV-Visible spectrophotometer (Perkin Elmer Model Lambda 35). For this, samples were placed in the path of one of the two light beams while a clean substrate (i.e. bare glass slide) in the other of reference.

Measurements essentially involve sequential recording of the intensities of two transmitted beams (through the sample and the reference) and displaying of the difference, as the transmittance (T) of the sample. The measurements were made at nominal incidence only.

Semiconductor devices composed of a thin film of ZnO on various substrates like glasses, Al_2O_3, Silicon dioxide on silicon and on silicon. Since certain electrical properties are dependent on film thickness, it is necessary to have a rapid, accurate and non-destructive means of measuring the film thickness. A convenient method has been described by Carl and Wimpfheimer (1).

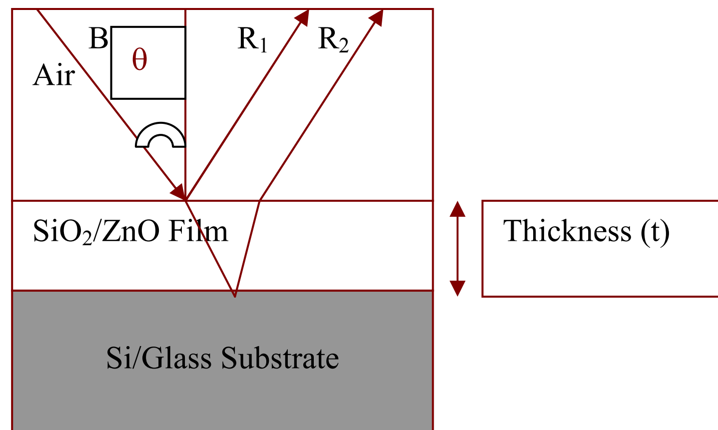

Figure 3.3: Ray diagram for optical reflection

Theory

The method used for measuring film thickness is called the interference fringe technique. It has been applied to both infrared and ultraviolet-visible spectroscopy.

In theory the phenomenon is quite simple. A beam of incident light (B) strikes the zinc oxide film layer at an angle α (see in the fig.). A portion of the beam is reflected (R_1) by

the film layer surface. The remainder of the beam is refracted by the film, reflected at the interface of the film and the substrate and emerges as beam (R_2). The combined intensity of the net resultant ray at a given wavelength is a function of the phase difference between the two beams at the given wavelength.

When the wavelength of light striking a ZnO layer, having uniform thickness, is continuously varied using a scanning double-beam spectrophotometer, the resulting spectrum is a continuous series of waves (maxima and minima). These maxima and minima are caused by the alternate reinforcement, at certain wavelength produces the maxima and minima, while destructive interference, or cancellation, causes the minima. The resulting spectrum is a series of interference fringes. It can be shown that the film thickness (t) is a function of:

λ_1= a convenient maximum wavelength

λ_m= a convenient minimum wavelength

n= the index of refraction

N= the number of fringes between λ_m and λ_1

α= the angle of incidence

The relationship used to express film thickness is expressed:

$$t= [N (\lambda_1\lambda_m) C] / [2(\lambda_1-\lambda_m) (N^2-\sin^2\alpha)^{1/2}] \ldots\ldots\ldots\ldots (1.5)$$

Where a factor C has been introduced to yield a film thickness in Angstroms (A^0), assuming wavelength is expressed in nanometers.

C =10 A^0/nm (conversion factor)

The band-gap of the of the thin film can be calculated by the following formula;

$$E_g=hc/\lambda \ldots\ldots\ldots\ldots\ldots\ldots\ldots\ldots\ldots\ldots\ldots\ldots (1.6)$$

Where λ is the absorption edge of the transmission spectra.

Limitation of the method

1. The primary limitations of the method are;
2. A lower thickness limit of $1000A^0$ (or 0.1μm);
3. Purity of film and surface condition; and
4. Variation of refractive index with wavelength.

Advantages of the method

This method offers a rapid, accurate, and non-destructive method for the determination of the thickness of the thin films. Carl and Wimpfheirmer (1) demonstrate the excellent correlation between the UV-VIS interference method, the weighing method, and the double beam interferometer method**.** Only the UV-VIS interference method is non-destructive.

2.3.3 Atomic force microscopy (AFM)

As the demand for smaller and faster products increases, characterization methods that are faster and more precise must also improve. Atomic force microscopy (AFM) is commonly used to characterize surface topography of given samples. Technologies affecting the electronics, biological, chemical, and automotive industries use the AFM to solve processing and materials problems. The materials being investigated include thin and thick film coatings, semiconductors, ceramics, metals, micro-mechanical properties of biological samples, nucleic acids, DNA and RNA, polymers and biomaterials, to name a few.

The AFM has made it possible to obtain 3-dimensional images of surfaces down to the atomic scale as well as to measure forces up to nano-Newton scale. The working components of the AFM are continually evolving. Work in this thesis focuses on one such area that will potentially improve the speed and preciseness of imaging surfaces of samples.

AFM background

Binning, Quate and Gerber invented atomic Force Microscopy (AFM) in 1986. Today, most AFMs use a laser beam detection system, which is shown schematically in Fig. 3.4. In this optical AFM, a laser beam is reflected from the back surface of a cantilever beam onto a position-sensitive photodiode. The photodiode is divided into four quadrants. When the cantilever is not interacting with the sample, the laser is positioned at the center of the photodiode as a reference point. When the sharp tip of the cantilever beam comes in close contact with the sample the cantilever beam bends in response to the forces between the tip and the sample which causes the laser beam to shift its position on the photodiode. As a result, one quadrant of the photodiode will be illuminated more than

another. By measuring the difference in light intensities between the upper and lower portions of the photodiode, a differential signal (A-B) is created and converted to a voltage signal. This signal is used in a control feedback loop to help maintain a constant force between the tip and the sample as the beam is raster scanned across the sample surface.

The sample typically sits on a positioning device made from piezoelectric ceramics. This positioning device, usually a tube scanner, is capable of sub-angstrom resolution in the x-, y-, and z-directions. Motion in the x- and y-directions typically performs the raster movement. Surface mapping is usually accomplished by maintaining a constant force between the tip and sample by moving the sample up and down with the help of a computer controlled feedback system. When the tip passes over a bump in the surface, the tip-sample separation becomes smaller which causes the cantilever to feel a force thereby bending the cantilever upward. The photodiode detects the detection, converts the detection to a voltage signal and adjusts the tip-sample separation by sending the signal to the z-piezo via the feedback system until the cantilever no longer experiences a detecting force. The voltages used to maintain constant tip-sample forces are converted to distances and used to obtain the 3-dimensional image.

Force curve

The radius of curvature of the very end of the cantilever tip can be ~ 10 nm. The very sharp tip means that only a few atoms are involved in the tip-sample interaction and the forces between the tip and sample are governed by the intermolecular force curve shown in Fig. 3.5. At the right side of the curve, the tip and sample are separated by a large distance and no force is experienced. As the atoms between the tip and sample are brought together, they first weakly attract each other. This attraction increases until the atoms are so close together that their electron clouds interact and begin to repel each other. The repulsive force continually weakens the attractive force as the distance decreases. When the distance between the atoms is a few angstroms, the force goes to zero. As the force becomes positive, the atoms between the tip and the sample come into contact with each other. The interaction between the tip and the sample is important when talking about the different modes of operation.

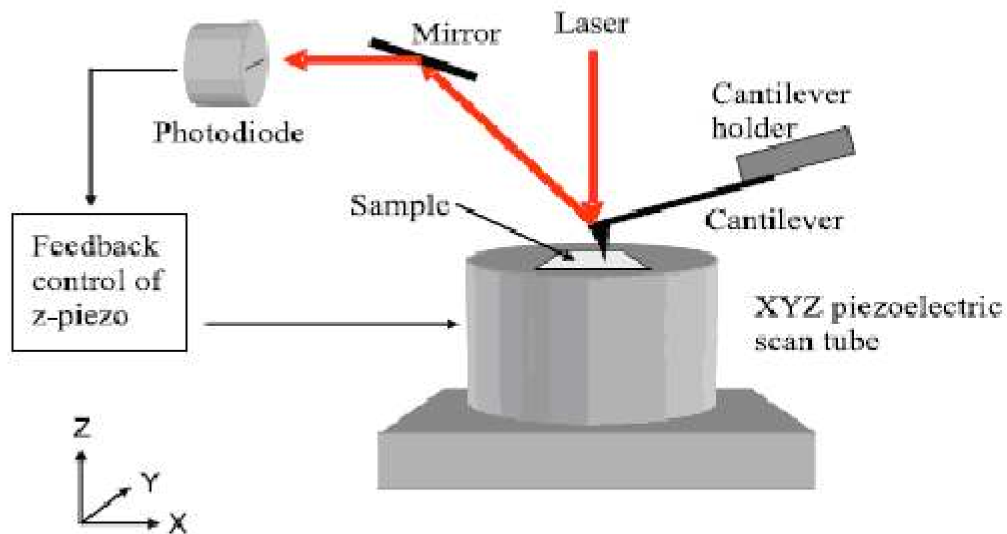

Figure 3.4: Schematic of atomic force microscope (AFM).

AFM modes of operation

There are three commonly used modes of operation in the AFM: contact mode, non-contact mode and tapping mode.

Contact mode

In contact mode operation, as the name implies, the tip is in close contact with the sample surface as it is scanned over the sample. The force on the tip is in the repulsive regime of the inter-molecular force curve. By operating in the repulsive regime, high-resolution images are obtained because the forces in this region are greater than in the attractive region. The main drawback to the contact mode of operation is that large lateral forces exist on the sample as the tip is dragged across the surface, damage to the tip as well as the sample is possible.

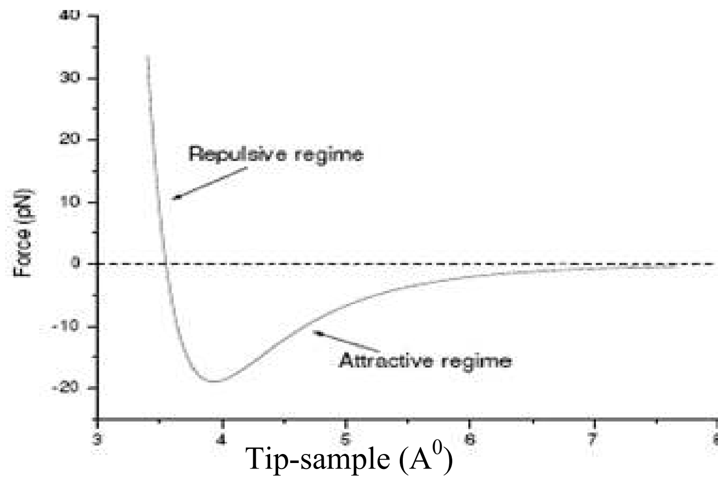

Figure 3.5: Intermolecular force curve.

Non-contact mode

In non-contact mode operation, the tip of the cantilever hovers above the sample surface. Attractive forces are the dominant forces between the tip and the sample. Forces in the attractive region are significantly weaker than forces in the repulsive region and, therefore, small oscillations are given to the tip of the cantilever via a dither piezoelectric crystal located within the cantilever holder. The forces between the tip and the sample are detected by measuring changes in amplitude, phase or frequency of the oscillating cantilever.

Tapping mode

In tapping mode operation, the tip of the cantilever is oscillated at or near the cantilever's resonant frequency and taps the surface of the sample. The tip of the cantilever comes into contact with the sample surface for very brief periods of time. By operating in the repulsive regime, high resolution is obtained, yet, the short duration of time that the cantilever is in contact with the sample limits the amount of damage associated with contact mode. The cantilever is driven at or near its resonant frequency by a dither piezoelectric crystal located within the cantilever holder. During scanning, the tip of the cantilever typically oscillates at a frequency of about 50-500 kHz. As the tip comes in intermittent contact with the sample, the amplitude of oscillation is reduced due to energy loss. The reduction in oscillation amplitude is used to identify and measure surface features.

Chapter –3

Results and Discussion

3.1 X-ray analysis

The crystal structure and orientaion of synthesized thin film were investigated by X-ray Difractrometer. The X-ray diffraction patterns of various samples of ZnO thin films has been recorded using Ritch-sefert X-ray diffractometer (model ISO Deby film 2002) with CuK_α radiation of wavelength 1.5418 A^0 and Rigaku model Geiger diffractogram with CuK_α radiation (λ = 1.5418 Å) obtained from the copper target using an in built Ni filter (at TCIRD). The X-ray diffraction pattern of ZnO thin film shown in the figures below indicate that the film is polycrystalline in nature and the crystallinity improves with increase in annealing temperature. XRD data was also indexed with JCPDS file (01-1136) of ZnO phase. The better crystallinity is obtained at annealing temperature of 600^0C. The X-ray diffraction pattern of the crystalline ZnO thin film reveals the existence of a ZnO single-phase with a hexagonal wurtzite structure.

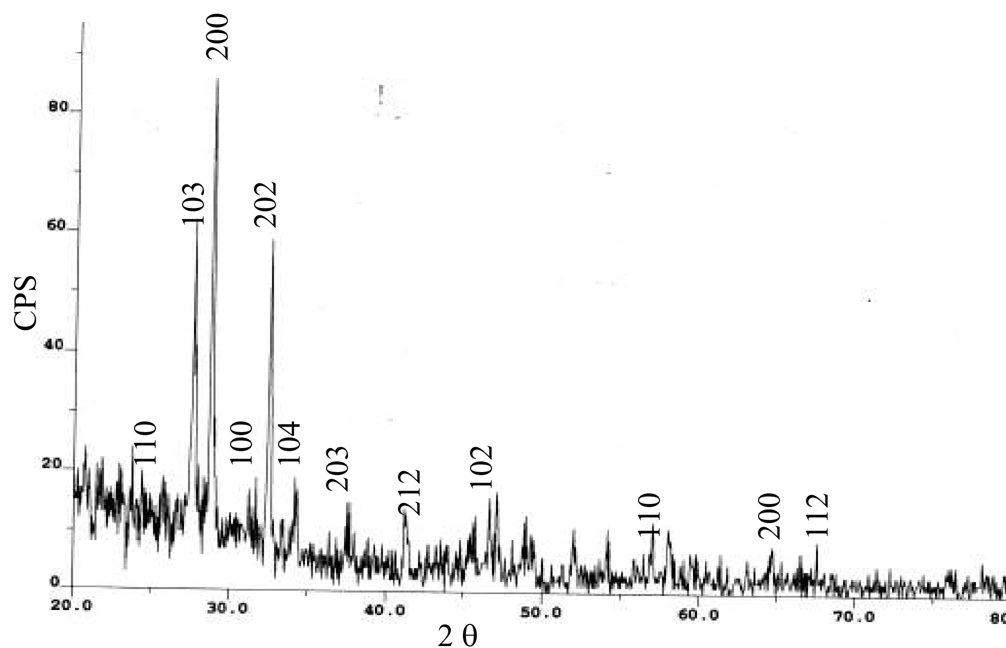

Figure 3.6: XRD pattern of ZnO annealed at 600^0C

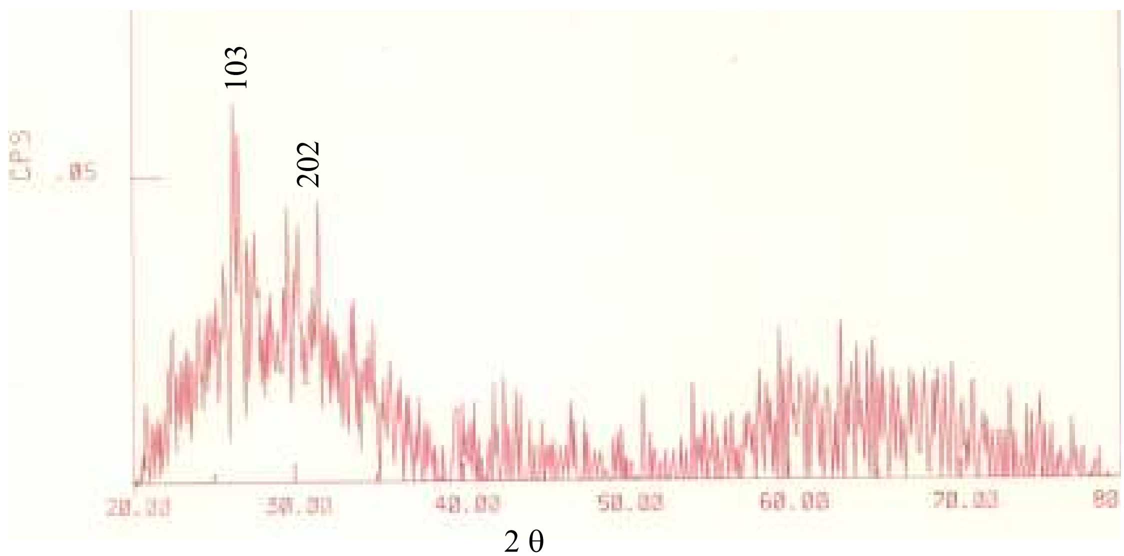

Figure 3.7: XRD pattern of ZnO annealed at 550^0C

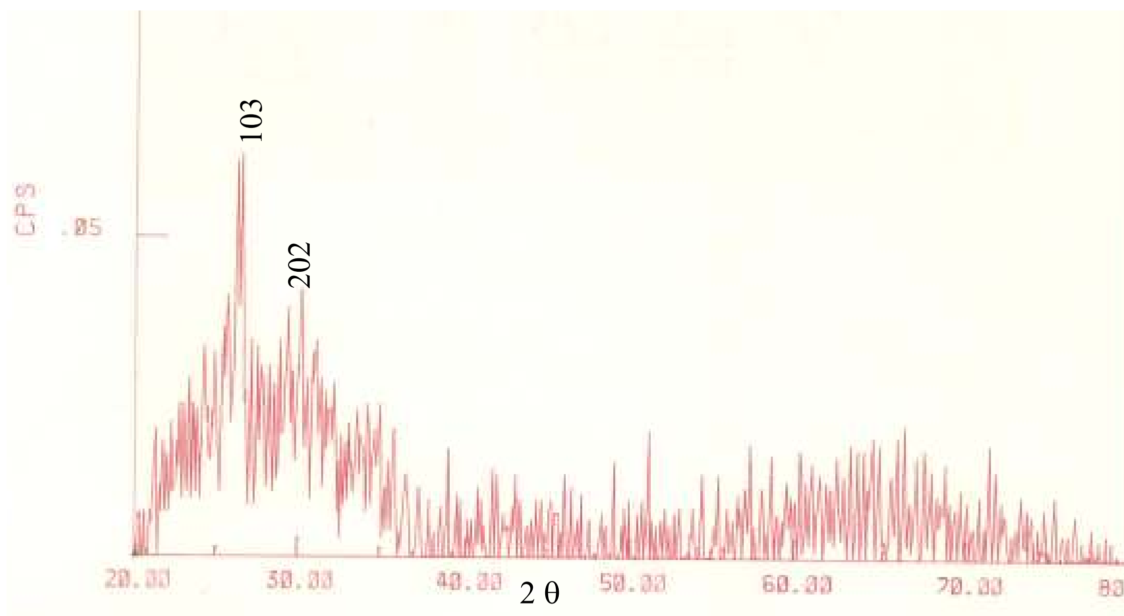

Figure 3.8: XRD pattern of ZnO annealed at 500^0C

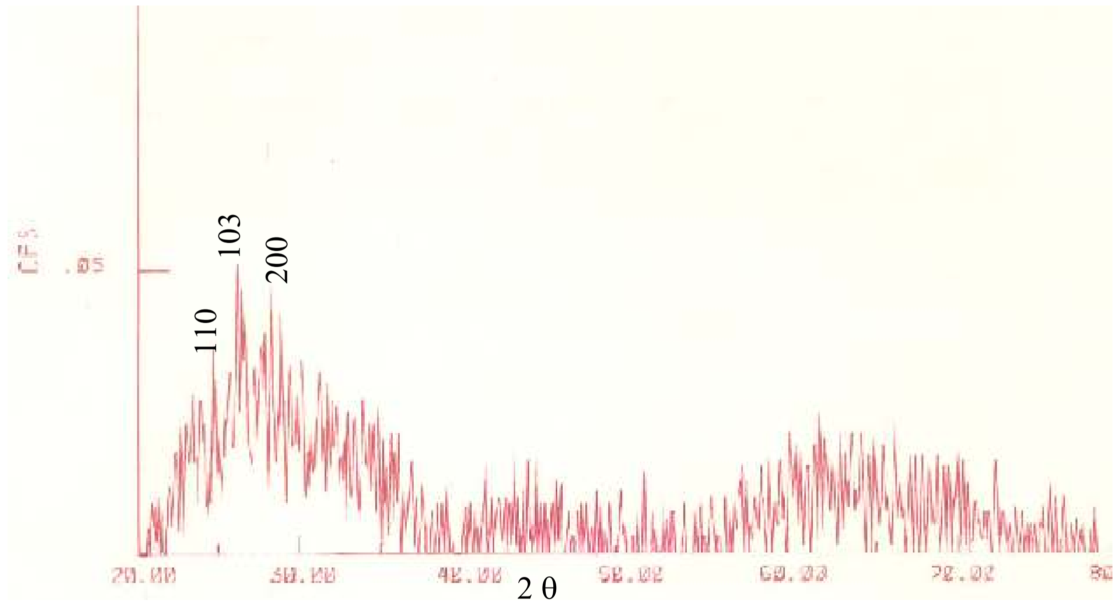

Figure 3.9: XRD pattern of ZnO annealed at 450^{0}C

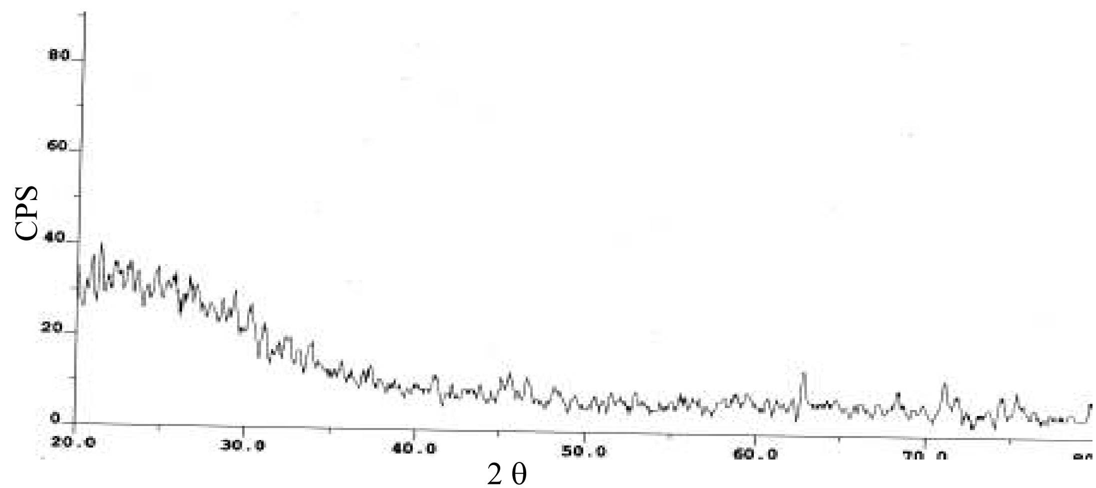

Figure 4.0: XRD pattern of ZnO thin film of as grown at 27^{0}C

3.2 UV-VIS spectrophotometer analysis

Optical transmittance (T) of ZnO thin film was measured in the wavelength range of 250-500nm with the UV-Visible spectrophotometer (Perkin Elmer Model Lambda 35). The UV-VIS spectra of ZnO thin film shows that the absorption peak is found at 382.79nm and the transmittance of both the spectra are different i.e 4.75% at 500^{0}C and 6.28% at

600^0C on the absorption peak. The nano-structured ZnO thin film has wavelength at absorption edge near 380nm.

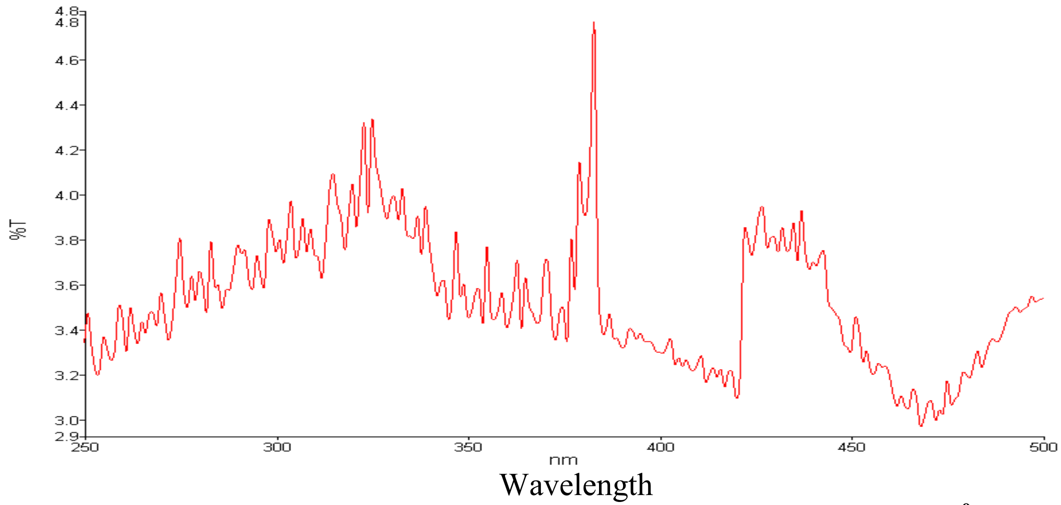

Figure 4.1: UV-VIS spectra of ZnO thin film at 500^0C

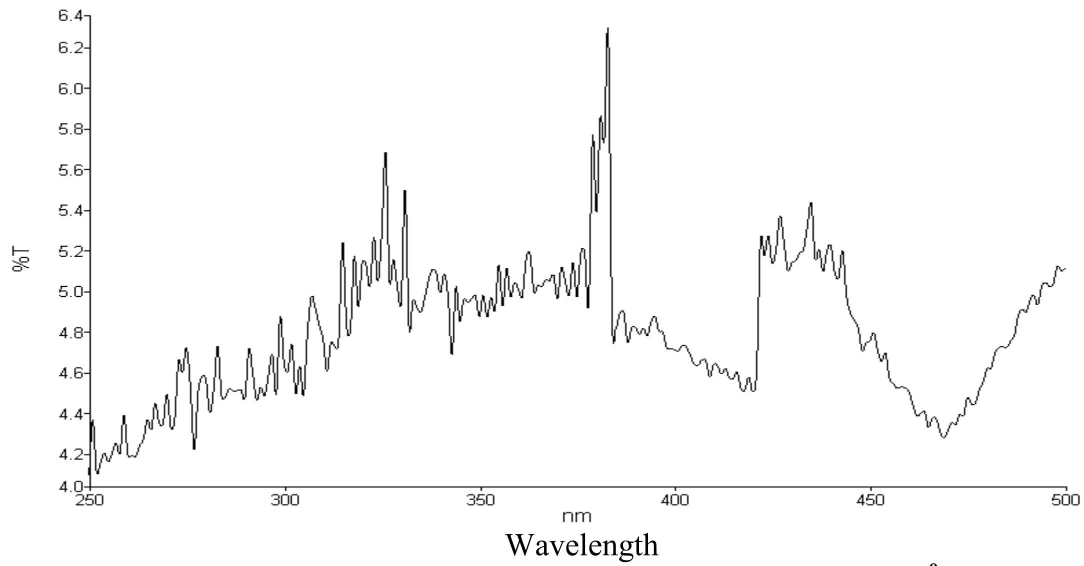

Figure 4.2: UV-VIS spectra of ZnO thin film at 600^0C

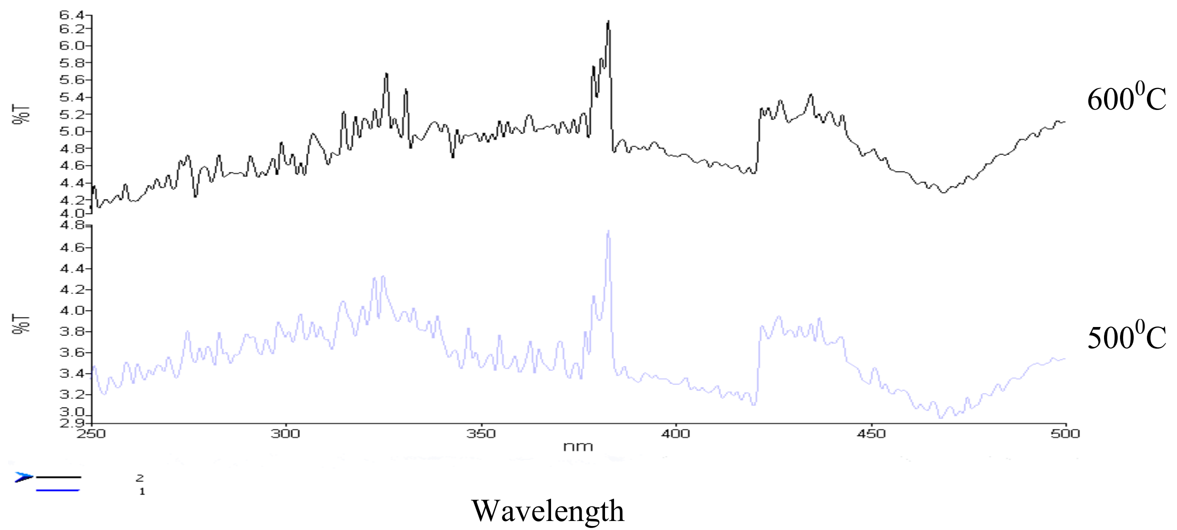

Figure 4.3: Comparison of UV-VIS spectra of ZnO thin film at both the temperatures

At all the annealing temperatures, the UV-VIS has the same spectra and the value of transmittance increases with the annealing temperature and maximum at 600^{0}C. The thickness of the film is calculated by using eq. 1.5. The thickness of the ZnO thin film is 334.09nm that is average value shown by the AFM image of ZnO thin film. The band gap of the ZnO thin film was calculated from eq.1.6. The value of band gap was found to be 3.25eV.

3.3 AFM analysis

The AFM spectra micrographs are shown in Fig 4.4 at different annealing temperatures. The micrographs reveals that adhesion property improves with increase in annealing teperatures. The AFM image shows the surface roughness changed with annealing temperatures.

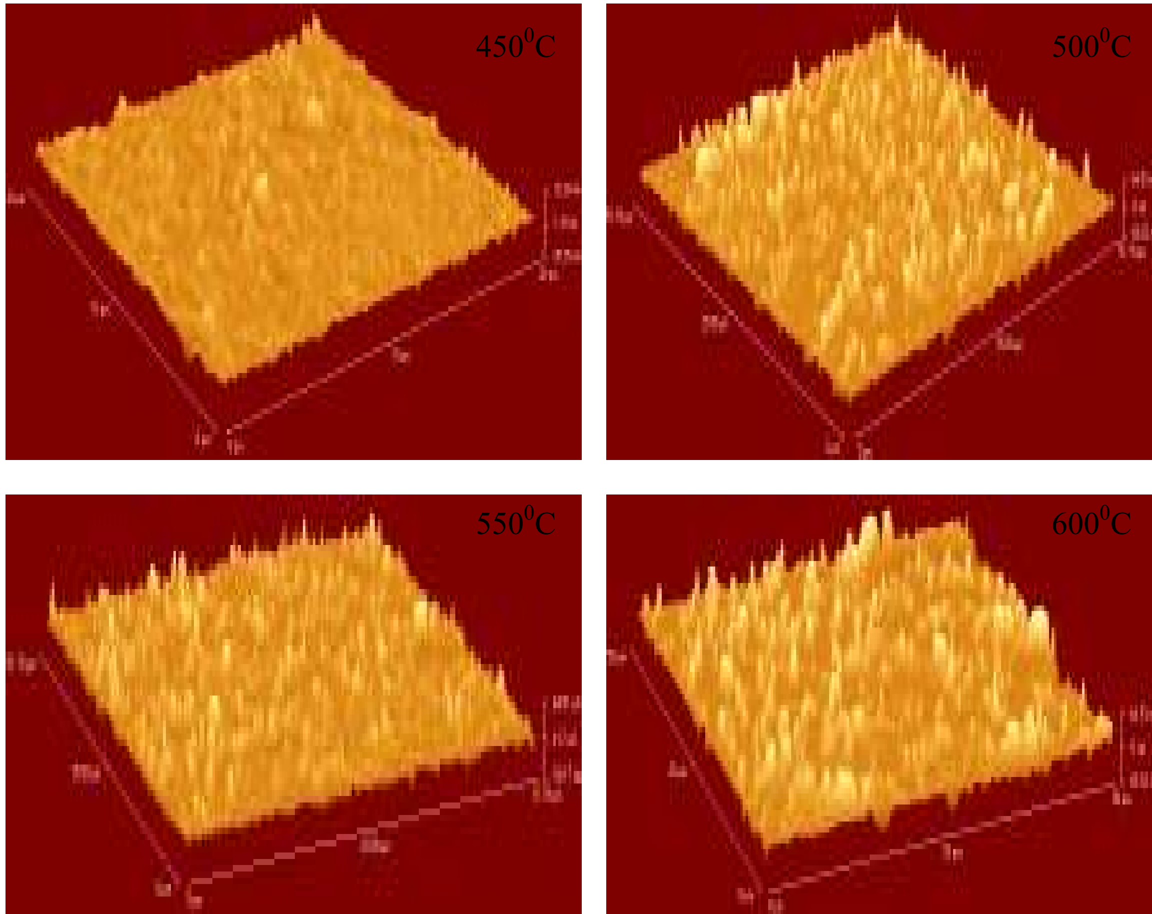

Figure 4.4: 3D AFM image of ZnO thin film annealed at different temperatures

The grain size depends on the number of applied pulses and on the substrate temperature of the substrate. The AFM characterization of ZnO thin films at different annealing temperatures revealed a granular, polycrystalline morphology with grain size increases with annealing temperatures.

Table 4: Grain Size of ZnO thin film measured by AFM image

ANNEALING TEMPERATURE (ºC)	GRAIN SIZE (μm)
450	0.16
500	1.00
550	1.05
600	2.56

The qualitative analysis of results via characteristics surface roughness R_a and deviation of Z direction on the sample surface are shown in the table below.

Table 5: Surface roughness of ZnO thin film measured by AFM

ANNEALING TEMPERATURE ºC	SURFACE ROUGHNESS			
	Area Roughness R_a (in nm)	Area RMS (in nm)	Average Height (in nm)	Maximum Range (in nm)
450	79.18	98.35	265.52	539.00
500	372.88	454.65	1243.52	2490.00
550	444.55	516.23	1207.09	2491.50
600	123.55	163.84	321.66	919.50

The area roughness R_a and the area RMS were found to be maximum at the annealing temperature 550 ºC.

The AFM data shows that the adhesion property improves with the annealing temperatures. The deflection in AFM cantilever is more at the interfacial layer of substrate and the ZnO thin film.

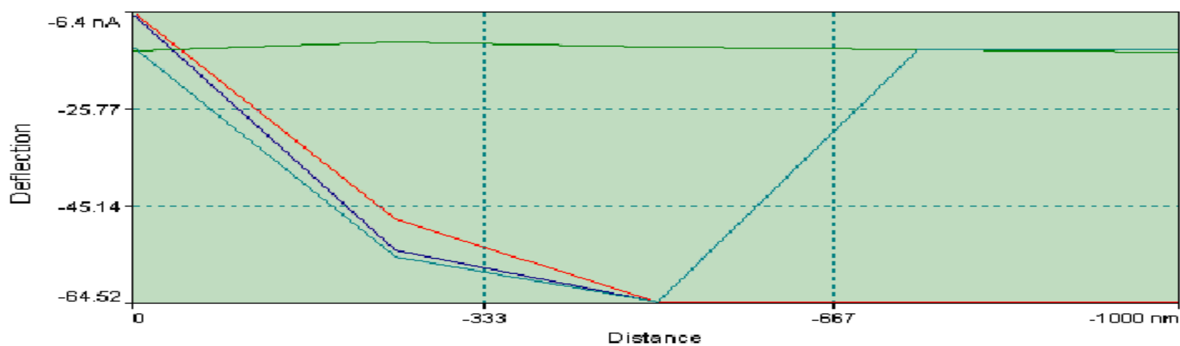

Figure 4.5(a): Force analysis at 600^0C

Figure 4.5(b): Force analysis at 600^0C

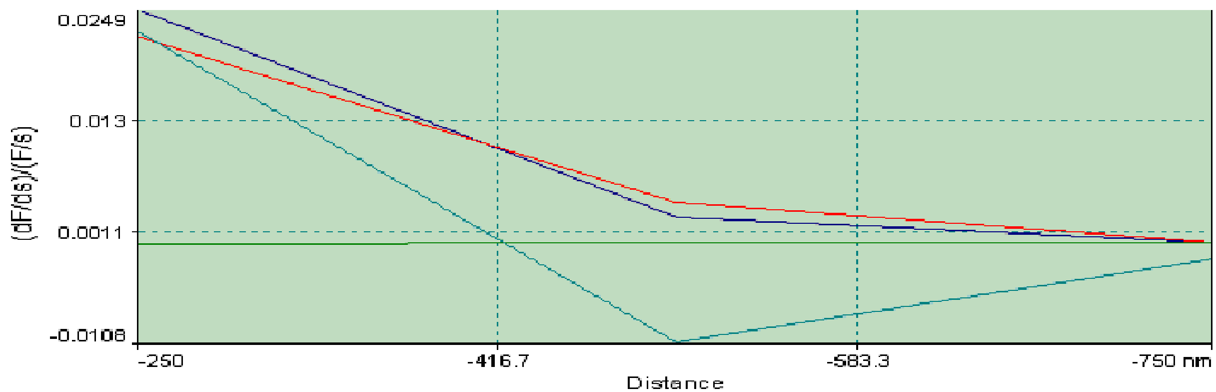

Figure 4.5(c): Force analysis at 600^0C

Fig 4.5 explains the adhesion property of the ZnO thin films at 600^0C at different points of the thin film. At the some points, the adhesion is so high and particles accumulate indicating different height. Adhesion improves with the annealing temperature and the surface roughness of the film decreases.

3.4 Conclusions

1. Thin films of ZnO were grown by thermal evaporation technique indicating these films were not fully transparent but should brownish color, indicating metallic nature of ZnO thin films. It is due to fact that ZnO decomposes at the evaporation temperature and thin films which have some oxygen deficiency. After annealing in the air, at different temperatures, the thin film becomes fully transparent and dense.

2. XRD analysis of the annealed thin films shows that, the crystallinity got with increase in annealing temperature and film was highly crystalline at 600^0C. The XRD pattern also explains that the existence of ZnO single phase with a hexagonal wurtzite structure.

3. UV-VIS spectrophotometer study reveals that;

1) The absorption peak was obtained at 382.79nm with transmittance of 4.75% (at 500^0C) and 6.28% (at 600^0C). This absorption peak matches with the theoretical value of ZnO nano-structured thin films.
2) The thickness of the film was 334.09nm.
3) The band gap of the ZnO thin film was 3.25eV, which is very close to the theoretical value of 3.3eV.

4. The AFM study reveals that;

1) The grain size was lowest to be 0.16μm at 450^0C (see in Table-4) and highest to be 2.56μm at 600^0C.
2) The surface roughness changes with annealing temperature and highest at 550^0C (R_a=444.56nm) with RMS value 516.23nm.
3) Adhesion property improves with annealing temperature and is maximum at 600^0C.
4) There is accumulation of particles at certain points. The adhesion is highest at these points and with maximum particle height.

3.5 Future Scope

Followings are the future scopes;

1) Since ZnO shows piezoelectric behavior, so it can be used as cantilever of AFM tip and for sensor applications.
2) ZnO is high band gap material, and hence it may be used in LED's.
3) The ZnO shows ferroelectricity at room temperature; hence it can be used in spintronic for memory applications.
4) Adhesion measurement of ZnO thin films can be done on the different substrate like SiO_2/Si, quartz, sapphire and Si.

References and Bibliography

1. K.L.Chopra, S.Major, D.K. Pandya, Thin Solid Films, **102** (1-46), 1 (1983).
2. H.L. Hartnagel, A.K. Dawar, A.K. Jain; Transparent Semiconducting Films, Institute of Physics, London (1995).
3. T. Nakada and N. Murakami, Transparent Conducting Al, AlB12 and B doped ZnO films for solar cells by DC Magnetron Sputtering, 12th European Photovoltaic Energy Conference **1507** (1994).
4. Milton Ohring, Materials Science of Thin Films; Deposition and Structure, **2**, Academic Press, (2002).
5. Donald L. Smith, Thin Film Deposition; Principal & Practice, Mc-Graw Hill,Inc., (1995).
6. Ryohei Kobayashi, Naoya Sato, Masaya Ichimura and Esuke Arai, 3rd conference on photovoltaic energy conversion, 11-18, 2003, Osaka, Japan.
7. F. Goto, M. Ichimura and E. Arai "A New Technique of compound Semiconductor deposition from an Aqueous Solution by Photochemical Reactions", Jpn. J. Appl. Phys.**36**, L1146 (1997).
8. S. Shishiyanu et al, "Synthesis and Characterization of Functional Nanostructured Zinc Oxide Thin Films, ECS Transactions, **39** 65-71 (2006).
9. N.I. Kovtyukhova et al, Ultrathin nanoparticle ZnS and ZnS: Mn films: surface sol–gel synthesis, morphology, photophysical properties, Elsevier Science S.A.; Mat. Sci. and Engg. B**69**, 411-417 (2000)
10. Katsumi Kushiya, Application of Stacked ZnO films as a window layer to Cu (InGa) Se2 Based Thin Film modules, Jpp. Appl. Phys., 38, 7A, 3997 (1997).
11. Dave Pier and Kim Mitchell, Effect of ZnO in ZnO/CdS/$CuInSe_2$ photovoltaic devices, 12th European Photovoltaic Energy Conference, **488**, (1994).
12. M. Amlouk and S. Belgacem, Effect of ZnO thin Layer on the photovoltaic characteristics of CdS/$CuInS_2$, 12th European Photovoltaic Energy Conference, **519**, (1994).
13. T. Yamamoto, Hisashi Kaga, Yoshiaki Kinemuch, Huseyin Yilmaz, KojiWatari, Hiromi Nakano, Hiroshi Nakano, Satoshi Tanaka, Atsushi Makiya, Zenji Kato

and Keizo Uematsu, Orientation dependence of transport property and microstructural characterization of Al-doped ZnO ceramics, J.Appl. Phys. **51**, 3113(1980).

14. Zhong Lin Wang, The new field of nano-piezotronics, Materials today, **10** 5 (2007).
15. Jun Zhou, Ningsheng Xu, and Zhong L. Wang, Adv. Mater., **0 3**, 1625 (2003).
16. Shunichi Hayamizu, Hitoshi Tabat, Hidekazu Tanaka and Tomoji Kawai, Preparation of Crystallized ZnO films on amorphous glass substrates by pulsed laser deposition, J. Appl. Phys. **80**, 2, 787 (1996).
17. Baosheng Sang, Akira Yamada and Makoto Konagai, Highly Satable ZnO thin Films by Atomic Layer Deposition, Jpn. J. Appl. Phys., **37**, 9A, L1125, (1998).
18. M. Amlouk and S. Belgacem, Effect of ZnO thin Layer on the photovoltaic characteristics of $CdS/CuInS_2$, 12th European Photovoltaic Energy Conference, **519**, (1994).
19. Ren-De Sun, Donald A. Tryk and Akira Fujishima, Adhesion of Electroless deposited Cu on ZnO-coated glass substrates: The Effect of the ZnO surface morphology, J. Electrochemical Society, **146** (6), 2117 (1999).
20. S.A. Studenikin, Nickolay Golego and Michael Cocivera, Optical and Electrical Properties of undoped ZnO films grown by Spray Pyrolysis of zinc nitrate solution, J. App. Phy., **83**(4), 2104 (1998).
21. Baosheng Sang, Akira Yamada and Makoto Konagai, Highly stable ZnO thin films by Atomic Layer Deposition, Jpn. J. Appl. Phys., **37**, 10A, 1125 (1998).
22. Wilson W. Wenas, Akira Yamada, Makoto Konagai and Kiyoshi Takahashi, Textured ZnO thin films for solar cells grown by MOCVD, Jpn. J. Appl. Phys., **30**, 3B, L441 (1991).
23. K. Ellmer, R. wendt, K. Diesner and S. Fiechter, Comparison of Different Deposition Methods for ZnO; Al films; Reactive Magnetran Sputtering from metallic Zn; Al targets (DC and RF) and from ZnO; Al_2O_3-targets(RF), 12th European Photovoltaic Energy Conference, 1515 (1994).

24. Vesa Lujala, Jarmo Skarp, Markku Tammenmaa, Tuomo Suntola and Jeike Wallinga, ZnO thin films for solar cells prepared by Atomic Layer Epitaxy, 12th European Photovoltaic Energy Conference, **1511** (1994).
25. Keiichiro Sakurai, Daiji Lwata, Shizuo Fujita and Shigeo Fujita, Growth of ZnO by Molecular Beam Epitaxy Using No_2 as Oxygen source, Jpn. J. Appl. Phys., **38**, 4B, 2606 (1999).
26. F. Hamdani, M. Yeadon, David J. Smith and H. Morkoo, Microstructure and Optical Properties of epitaxial GaN on ZnO (0001) grown by Reactive Molecular Beam Epitaxy, J. Appl. Phys., **83**, 2, 983 (1998).
27. Y. Cui. C.M. Lieber, Functional Nanoscale Electronic Devices Assembled Using Silicon Nanowire Building Blocks, Science, **291**, 851 (2001).
28. Yu Huang, Xiangfeng Duan, Qingqiao Wei, Charles M. Lieber, Directed Assembly of One-Dimensional Nanostructures into Functional Networks, Nature **409**, 66 (2001).
29. M.S. Gudiksen, L.J. Lauhon, J. Wang, D.C. Smith, C.M. Lieber, Thermal evaporation synthesis of zinc oxide nanowires, Nature. **415**, 616 (2002).
30. M. Ristov, Gj. Sinadinovski, I. Grozdanov and M. Mitreski, Chemical deposition of ZnO films, Thin Solid Films **149**, 65 (1987).
31. YJ Xing, ZH Xi, XD Zhang, JH Song, RM Wang, J Xu, Thermal evaporation synthesis of zinc oxide nanowires, Appl. Phys. **A 80**, 1527-1530 (2005).
32. Y. C. Kong, D. P. Yu, B. Zhang, W. Fang, and S. Q. Feng, Ultraviolet-emitting ZnO nanowires synthesized by a physical vapor deposition approach, Appl. Phys Lett. **78**, 407 (2001).
33. Michael H. Huang, Samuel Mao, Henning Feick, Haoquan Yan, Yiying Wu, Hannes Kind, Eicke Weber, Richard Russo, Peidong Yang, Room-Temperature Ultraviolet Nanowire Nanolasers, Science **292**, 1897 (2001).
34. Zhong Lin Wang, The new field of nanopiezoelectronics, Materials Today, **10**, 5, 20 (2007).
35. Harish Bahadur, S.C. Garg, et al., Preperation and characterization of ZnO thin films on silicon substrate using sol-gel process, Physics of Semiconductor Devices (IWPSD-2003), Narosa Publishing New Delhi, **12**, 298-300, (2003)